Published in final edited form as:

Evolution. 2019 December ; 73(12): 2368–2389. doi:10.1111/evo.13850.

Molecular evolution of the meiotic recombination pathway in mammals

Amy L. Dapper[1,2,3], **Bret A. Payseur**[1]

[1]Laboratory of Genetics, University of Wisconsin, Madison, Wisconsin 53706

[2]Department of Biological Sciences, Mississippi State University, Mississippi 39762

Abstract

Meiotic recombination shapes evolution and helps to ensure proper chromosome segregation in most species that reproduce sexually. Recombination itself evolves, with species showing considerable divergence in the rate of crossing-over. However, the genetic basis of this divergence is poorly understood. Recombination events are produced via a complicated, but increasingly well-described, cellular pathway. We apply a phylogenetic comparative approach to a carefully selected panel of genes involved in the processes leading to crossovers—spanning double-strand break formation, strand invasion, the crossover/non-crossover decision, and resolution—to reconstruct the evolution of the recombination pathway in eutherian mammals and identify components of the pathway likely to contribute to divergence between species. Eleven recombination genes, predominantly involved in the stabilization of homologous pairing and the crossover/non-crossover decision, show evidence of rapid evolution and positive selection across mammals. We highlight *TEX11* and associated genes involved in the synaptonemal complex and the early stages of the crossover/non-crossover decision as candidates for the evolution of recombination rate. Evolutionary comparisons to *MLH1* count, a surrogate for the number of crossovers, reveal a positive correlation between genome-wide recombination rate and the rate of evolution at *TEX11* across the mammalian phylogeny. Our results illustrate the power of viewing the evolution of recombination from a pathway perspective.

Keywords

Adaptive evolution; crossover; divergence; evolutionary rate; pathway evolution

Meiotic recombination, the reciprocal exchange of DNA between homologous chromosomes, during meiosis is a major determinant of genetic diversity in populations,

[3] dapper@biology.msstate.edu.

AUTHOR CONTRIBUTIONS

ALD and BAP designed the study. ALD collected the data and ran the analyses. ALD and BAP wrote the manuscript.

DATA ARCHIVING

Sources and accession numbers for all publicly available sequence data used in this study can be found in Tables S1– S3 and S7. All data, sequence alignments, and code necessary to replicate this study can be found in the following publicly available GitHub Repository: https://github.com/adapper/EvoRecGenesMS.

Supporting Information

Additional supporting information may be found online in the Supporting Information section at the end of the article.

influencing the fate of new mutations (Hill and Robertson 1966), the efficacy of selection (Felsenstein 1974; Charlesworth et al. 1993; Comeron et al. 1999; Gonen et al. 2017), and several features of the genomic landscape (Begun and Aquadro 1992; Charlesworth et al. 1994; Duret and Arndt 2008). Recombination is also required for successful gametogenesis in most species that reproduce sexually (Hassold and Hunt 2001).

Although recombination rate is often treated as a constant, this fundamental parameter evolves over time. Genomic regions ranging in size from short sequences to entire chromosomes vary in recombination rate—both within and between species (Burt and Bell 1987; Broman et al. 1998; Jeffreys et al. 2005; Coop and Przeworski 2007; Kong et al. 2010; Dumont et al. 2011; Smukowski and Noor 2011; Comeron et al. 2012; Segura et al. 2013; Dapper and Payseur 2017; Stapley et al. 2017). Despite important insights about the conditions that favor recombination rate evolution from theoretical work, the balance of evolutionary forces responsible for observed patterns of inter-individual variation in nature has rarely been examined (Dapper and Payseur 2017; Ritzetal.2017). For example, the form, intensity, and significance of natural selection as a driver of recombination rate evolution are unknown.

Discovering the genetic underpinnings of differences among individuals—including the numbers, genomic locations, and phenotypic effects of causative mutations and genes—provides a window into how recombination rate evolves. Genome-wide association studies are beginning to reveal the genetic basis of variation in recombination rate within species. Individual recombination rates have been associated with variants in specific genes in populations of *Drosophila melanogaster* (Hunter et al. 2016), humans (Kong et al. 2008, 2014; Chowdhury et al. 2009; Fledel-Alon et al. 2011), domesticated cattle (Sandor et al. 2012; Ma et al. 2015; Kadri et al. 2016; Shen et al. 2018), domesticated sheep (Petit et al. 2017), Soay sheep (Johnston et al. 2016), and red deer (Johnston et al. 2018). Variants in several of these genes correlate with recombination rate in multiple species, including *RNF212* (Kong et al. 2008; Chowdhury et al. 2009; Fledel-Alon et al. 2011; Sandor et al. 2012; Johnston et al. 2016; Kadri et al. 2016; Petit et al. 2017), *RNF212B* (Johnston et al. 2016, 2018; Kadri et al. 2016), *REC8* (Sandor et al. 2012; Johnston et al. 2016, 2018), *HEI10/CCNB1IP1* (Kong et al. 2014; Petit et al. 2017), *MSH4* (Kong et al. 2014; Ma et al. 2015; Kadri et al. 2016; Shen et al. 2018), *CPLX1* (Kong et al. 2014; Ma et al. 2015; Johnston et al. 2016; Shen et al. 2018) and *PRDM9* (Fledel-Alon et al. 2011; Sandor et al. 2012; Kong et al. 2014; Ma et al. 2015; Shen et al. 2018).

In contrast, we know very little about the genetics of recombination rate evolution between species. Divergence at the dicistronic gene *mei-217/mei-218* explains much of the disparity in genetic map length between *D. melanogaster* and *D. mauritiana* (Brand et al. 2018). *mei-217/mei-218* is the only gene known to confer a recombination rate difference between species, although quantitative trait loci that contribute to shifts in rate among subspecies of house mice have been identified (Murdoch et al. 2010; Dumont and Payseur 2011; Balcova et al. 2016).

Most of the genes that function in the cellular pathway that produces crossovers are known (see Table 1). Divergence in recombination rate likely traces back to mutations in these

genes. Therefore, one strategy for understanding how species diverge in recombination rate is to inspect patterns of molecular evolution at genes involved in the pathway that leads to crossovers. With this approach, the role of natural selection in the evolution of the pathway can be evaluated. *mei-217/mei-218* was targeted for functional analysis based on its profile of rapid evolution between *D. melanogaster* and *D. mauritiana* (Brand et al. 2018). *PRDM9*, a protein that positions recombination hot spots in house mice and humans through histone methylation (Myers et al. 2010; Parvanov et al. 2010; Grey et al. 2011; Paigen and Petkov 2018), shows accelerated divergence across mammals (Oliver et al. 2009). Although these examples demonstrate the promise of signatures of molecular evolution for illuminating recombination rate differences between species, patterns of divergence have yet to be reported for most genes involved in meiotic recombination. A profile of molecular evolution across a collection of recombination genes would provide new information about the evolutionary forces that shape recombination rate from the perspective of a well-defined cellular pathway.

Mammals offer a powerful system for dissecting the molecular evolution of the recombination pathway for several reasons. First, the evolution of recombination rate has been measured along the mammalian phylogeny (Dumont and Payseur 2008; Segura et al. 2013). Second, recombination rate variation has been associated with specific genes in mammalian populations (Kong et al. 2008, 2014; Chowdhury et al. 2009; Sandor et al. 2012; Ma et al. 2015; Johnston et al. 2016, 2018; Kadri et al. 2016; Petit et al. 2017; Shen et al. 2018). Third, laboratory mice have proven instrumental in the identification and functional characterization of recombination genes (de Vries et al. 1999; Baudat et al. 2000; Romanienko and Camerini-Otero 2000; Yang et al. 2006; Ward et al. 2007; Schramm et al. 2011; Bisig et al. 2012; Bolcun-Filas and Schimenti 2012; La Salle et al. 2012; Kumar et al. 2015; Finsterbusch et al. 2016; Stanzione et al. 2016).

Work in mice indicates that the mammalian recombination pathway is roughly divided into six major steps, each regulated by a handful of genes (Table 1). The first step is the formation of hundreds of double-strand breaks (DSBs) throughout the genome (Keeney et al. 1997; Bergerat et al. 1997; Baudat et al. 2000; Romanienko and Camerini-Otero 2000; Baudat and de Massy 2007; Finsterbusch et al. 2016; Lange et al. 2016). After formation, DSBs are identified, processed, and paired with their corresponding location on the homologous chromosome through homology searches and strand invasion (Keeney2007; Cloud et al. 2012; Brown and Bishop 2014; Oh et al. 2016; Kobayashi et al. 2016; Finsterbusch et al. 2016; Xu et al. 2017). The pairing of homologous chromosomes is then stabilized by a proteinaceous structure referred to as the synaptonemal complex (SC) (Meuwissen et al. 1992; Schmekel and Daneholt 1995; Costa et al. 2005; de Vries et al. 2005; Hamer et al.2006;Yang et al.2006; Schramm et al. 2011; Fraune et al. 2014; Hernández-Hernández et al. 2016).´ The SC also forms a substrate on which the eventual crossover events will take place (Page and Hawley 2004; Hamer et al. 2008). It is at this point that a small subset of DSBs is designated to mature into crossovers, leaving the majority of DSBs to be resolved as non-crossovers (Snowden et al. 2004; Yang et al. 2008; Reynolds et al. 2013; Finsterbusch et al. 2016; Rao et al. 2017). Finally, this designation is followed, and each DSB is repaired as a crossover or a non-crossover (Baker et al. 1996; Edelmann et al. 1996; Lipkin et al. 2002; Rogacheva et al. 2014; Xu et al. 2017).

The structure of the recombination pathway suggests that two steps play primary roles in determining recombination rate: (1) the formation of DSBs, and (2) the crossover/non-crossover decision. Although estimated numbers of DSBs and crossovers are positively correlated across species of bovids (Ruiz-Herrera et al. 2017), a key regulatory aspect of meiotic recombination predicts that recombination rate evolution results disproportionately from changes to the crossover/non-crossover decision. In mice, the total number of crossovers is relatively robust to changes in DSB number, a phenomenon referred to as crossover homestasis (Cole et al. 2012). Accordingly, if divergence in recombination rate is driven by directional selection across mammals (i.e., Segura et al. 2013), we expect to observe higher rates of molecular evolution and stronger signatures of positive selection in genes regulating the crossover/non-crossover decision compared to genes in other steps of the pathway. Conversely, if recombination rate is largely subject to purifying selection, we would expect to observe higher conservation among genes involved in the crossover/non-crossover choice. In particular, genes responsible for DSB formation could experience a relaxation of selection because their influence on recombination rate is buffered. Consistent with the expectation that crossover/non-crossover decision primarily regulates recombination rate, many of the genes identified as contributing to standing variation in recombination rate function late in the recombination pathway. If these genes contribute disproportionately to differences between species, we expect them to exhibit elevated rates of molecular divergence compared to other genes in the pathway.

In this article, we examine the molecular evolution of 32 key recombination genes, evenly distributed across each major step in the recombination pathway, across 16 species of mammals. We ask: (1) Do genes in the recombination pathway exhibit patterns of rapid and adaptive evolution across the mammalian phylogeny? (2) If so, are those genes concentrated in steps of the recombination pathway that regulate the crossover/non-crossover decision? (3) Do genes previously associated with population-level variation in recombination rate show elevated rates of evolution between species? (4) Are changes in the rate of molecular evolution correlated with genome-wide recombination rate?

Materials and Methods

DATA ACQUISITION AND PROCESSING

We selected a focal panel of 32 recombination genes (see Table 1). The panel was carefully selected to allow us to test hypotheses concerning the evolution of the recombination pathway. To identify differences in the rate of evolution between pathway steps, we selected representative genes that covered each major step as evenly as possible, focusing on genes with well-described, integral functions (e.g., *SPO11* catalyzes DSB formation). We also included genes that have been associated with inter-individual differences in recombination rate within mammalian populations (e.g., *RNF212*) to test the hypothesis that these genes are more likely to contribute to divergence between species.

For each gene, reference sequences from 16 species of mammals were downloaded from both NCBI and Ensembl (Release89) (Wheeler et al. 2006; Zerbino et al. 2017). These 16 species were selected using the following criteria: (1) availability of high-quality sequences for recombination genes, (2) availability of testes expression datasets, (3) availability of

estimates of recombination rate, and (4) coverage of a range of divergence times, without saturation at synonymous sites.

Alternative splicing is widespread and presents a challenge for molecular evolution studies (Pan et al. 2008; Barbosa-Morais et al. 2012). To focus our analyses on coding sequences that are transcribed during meiosis and to validate the computational annotations for each gene in each species, we used available testes expression datasets. Meiotic recombination occurs in adult testes and fetal ovaries. Transcripts present in these tissues are likely to represent the most relevant isoform. We relied entirely on testes expression datasets because fetal ovary expression datasets were not available. We downloaded raw testes expression data for each species from NCBI Gene Expression Omnibus (GEO) (Table S1) (Barrett et al. 2012). We converted the SRA files into FASTQ files using SRAtoolkit (Leinonen et al. 2010). The reads were mapped to an indexed reference genome (Tables S2 and S3) (Bowtie2; Langmead and Salzberg 2012) using TopHat (Trapnell et al. 2009). The resulting bam files were sorted using Samtools (Li et al. 2009) and visualized using IGV 2.4.10 (Thorvaldsdóttir et al. 2013). We used this approach to (1) identify the transcript expressed in testes, (2) check the reference transcript for errors, and (3) revise the reference transcript based on the transcript data.

We compared expression data to annotations from both Ensembl and NCBI (Wheeler et al. 2006; Zerbino et al. 2017). When both transcripts were identical, we selected the NCBI transcript. The Ensembl transcript was used instead when (1) the NCBI reference sequence was not available, (2) none of the NCBI transcripts matched the expression data, or (3) there were sequence differences between the two transcripts and the Ensembl transcript was more parsimonious (i.e., had the fewest differences when compared to the rest of sequences in the alignment). The use of testes expression data was a key quality control step. We found frequent errors in isoform annotation. The transcripts of each gene identified via testes expression dataset were highly concordant across species, further validating this approach. The inclusion of species in this study was primarily determined by the availability of testes expression data.

PHYLOGENETIC COMPARATIVE APPROACH

For each gene, we used phylogenetic analysis by maximum like-lihood (PAML 4.8) to measure the rate of evolution across the mammalian phylogeny and to search for molecular signatures in dicative of positive selection (Table 2) (Yang1997,2007). This approach requires a sequence alignment and a phylogenetic tree. For each gene, sequences were aligned using Translator X, a codon based alignment tool, powered by MUSCLEv3.8.31 (Edgar 2004; Abascal et al. 2010). Each alignment was examined by hand and edited as necessary. We used a species tree that reflects the current understanding of the phylogenetic relationships of the species included in our study (Fig. 1) (Prasad et al. 2008; Perelman et al. 2011; Fan et al. 2013; Chen et al. 2017; Letunic and Bork 2019).

Due to the ambiguity in the relationship between Laura-sithians and the placement of tree shrews, we also inferred gene trees using MrBayes (Ronquist et al. 2012; Fan et al. 2013; Chen et al. 2017). To infer each gene tree, we selected the general time reversible (GTR) substitution model with gamma-distributed rate variation across sites and the Markov chain

Monte Carlo (MCMC) sampling was run until the standard deviation (SD) frequency was less than 0.01 (Ronquist et al. 2012). We used this approach to account for effects of incomplete lineage sorting (ILS) (Pamilo and Nei 1988; Rosenberg 2002; Scornavacca and Galtier 2017). Using gene trees and using the consensus species tree produced highly similar results (Table S4).

For 19 genes, transcripts from all 16 species were used. For 11 genes in which the chimpanzee and bonobo sequences were identical, we excluded the bonobo sequence, as required by PAML 4.8 (Yang 1997, 2007). For one gene in which the chimpanzee, bonobo, and human sequences were all identical, we excluded the chimpanzee and bonobo sequences. In only two cases, a suitable reference sequence could not be identified for a given species (*RNF212B*: rat; *TEX11*: tree shrew).

We estimated rates of synonymous and nonsynonymous substitutions per site using the CODEML program in PAML 4.8 (Yang 2007). This program considers multiple substitutions per site, variation in the rate of transitions and transversions, and effects of codon usage (Yang 2007). Rates of substitution were computed for six different models of molecular evolution (Table 2). The fit of each model was compared using a likelihood ratio test. Reported substitution rates assume the best-fit model for each gene.

IDENTIFYING SIGNATURES OF SELECTION

To test for positive selection, we compared the fit of models including a class of sites with $\omega > 1$ to the fit of models in which all classes of sites have $\omega \leq 1$. Specifically, we report three comparisons: Model 1 versus Model 2, Model 7 versus Model 8, and Model 8 versus Model 8a (Table 2). The first comparison, M1 versus M2, compares a model with two classes of sites ($\omega < 1$, $\omega = 1$) to a model with a third class of sites where $\omega > 1$, indicative of positive selection (Yang 2007). More complex models (M7 and M8) were developed to consider variation in $\omega < 1$ among sites within genes by including 10 site classes drawn from a beta distribution ranging from 0 to 1 (Yang 2007). In this case, Model 8 includes one additional class of sites in which $\omega > 1$ (for a total of 11 site classes), allowing for the identification of signatures of positive selection (Yang 2007). In cases in which a large fraction of sites within a gene are evolving neutrally ($\omega = 1$), Model 8 will fit significantly better due to a very poor fit of Model 7 rather than a signature of positive selection. To avoid incorrectly identifying signatures of positive selection in this case, we also compared Models 8–8a, which contains a larger fraction of neutrally evolving sites than Model 7 (Swanson et al. 2003). We report the number of codons in each gene estimated to have $\omega > 1$ (Bayes empirical Bayes, BEB; $P > 0.95$).

MULTINUCLEOTIDE MUTATIONS

Multinucleotide mutations (MNMs) occur when two mutations happen simultaneously in close proximity (Schrider et al. 2011; Besenbacher et al. 2016). MNMs violate the PAML assumption that the probability of two simultaneous mutations in the same codon is zero (Yang 2007; Venkat et al. 2018). Recent work has shown that MNMs can lead to the false inference of positive selection when using branch-site tests in PAML (Venkat et al. 2018). Although we did not use branch-site tests, it is possible that MNMs contributed to some of

the signatures of positive selection we observed. Although we could not directly identify MNMs in our dataset, we conducted an additional analysis to gauge the potential effects of MNMs on our results. We used PAML to reconstruct the ancestral sequence at each node in the phylogeny (Yang 2007). For the reconstruction, Model 8 was chosen because we specifically reanalyzed genes that showed evidence for positive selection when comparing Model 7 with Model 8. From the ancestrally reconstructed sequences, we identified any codons in which PAML inferred more than one substitution on a single branch (codons with multiple differences; CMDs). All identified CMDs were removed from the sequences in which they occurred. For example, if a CMD was identified in an external branch, that codon was replaced with—only in the sequence of that species. If a CMD was inferred on an internal branch, the codon was replaced with—in all species descended from that internal branch. For each gene that showed evidence of positive selection using the unedited sequences, we also conducted PAML analyses using sequences from which all CMDs were removed.

POLYMORPHISM AND DIVERGENCE IN THE PRIMATE LINEAGE

To further examine evidence for selection on recombination genes, we compared divergence between humans and macaque to polymorphism within humans in the recombination genes. We chose the macaque–human comparison because the moderate levels of protein divergence between this pair of species is expected to provide good power for detecting signatures of selection (Gradnigo et al. 2016). Human polymorphism data were downloaded from ExAC database (Lek et al. 2016). The ExAC database spans 60,706 unrelated individuals sequenced as part of both disease-specific and population genetic studies (Lek et al. 2016). To avoid biases introduced by population structure, we restricted our analyses to the population with the largest representation in the database: European, non-Finnish, individuals (N = 33,370) (Lek et al. 2016). We also conducted complementary analyses that were restricted to individuals of African descent (N = 5,203) to ensure that the demographic history of European populations did not bias our results. The results from both populations were highly concordant (Table S5). Polymorphism data for the correct transcript of *RNF212* (based on expression data) was not available in the ExAC database; this gene was not included in this analysis.

We compared counts of nonsynonymous and synonymous polymorphisms to counts of nonsynonymous and synonymous substitutions using the McDonald–Kreitman test (McDonald and Kreitman 1991). The neutral expectation is that the ratio of non-synonymous to synonymous substitutions is equal to the ratio of nonsynonymous to synonymous polymorphisms (McDonald and Kreitman 1991). Significant deviations provide evidence of natural selection. The neutrality index (NI) measures the direction and degree of departures from the neutral expectation (Charlesworth et al. 1994). An $NI < 1$ indicates positive selection, and the fraction of adaptive amino acid substitutions can be estimated as $1 - NI$ (Charlesworth et al. 1994; Fay et al. 2001; Smith and Eyre-Walker 2002). We also measure the direction of selection (DoS) for each gene, an additional statistic that estimates the direction and degree of departures from the neutral expectation and has been shown to be less biased than NI under certain conditions (Stoletzki and Eyre-Walker 2010). A positive DoS is consistent with positive selection; a negative DoS indicates purifying selection

(StoletzkiandEyre-Walker2010). Additionally, we estimated pairwise divergence (ω) between human and macaque using the yn00 package in PAML (Yang 2007) (Table S6).

IDENTIFYING EVOLUTIONARY PATTERNS

To identify evolutionary patterns among recombination genes, we compared the rate of evolution and the proportion of genes experiencing positive selection among groups of interest. All statistical analyses were performed in R (R Core Team 2015).

EVOLUTIONARY RATE COVARIATION

To determine whether recombination genes coevolve, we computed the evolutionary rate covariation (ERC) metric: the correlation coefficient between branch-specific rates among pairs of proteins (Clark et al. 2012). ERC is frequently elevated among interacting proteins (Pazos and Valencia 2001; Hakes et al. 2007; Clark et al. 2009) and is assumed to result from (1) concordance in fluctuating evolutionary pressures, (2) parallel evolution of expression level, and/or (3) compensatory changes between coevolving genes (Clark et al. 2012, 2013; Priedigkeit et al. 2015). We used a publicly available ERC dataset (https://csb.pitt.edu/erc_analysis/index.php) to compare the median ERC-value among a subset of the focal recombination genes ($N = 25$) to other genes in the genome, as described in Priedigkeit et al. (2015).

To control for an observed elevation in ERC among recombination genes and test for relationships between specific groups, we also conducted an ERC analysis that was restricted to the focal set of 32 recombination genes. Branch lengths were calculated using the aaML package in PAML (Yang 2007) and pairwise ERC values were calculated following the methods of Clark et al. (2012). Using this approach, we specifically compared the ERC values among three of the most rapidly evolving recombination genes (*TEX11, SHOC1,* and *SYCP2*) to the other recombination genes.

To ask whether divergence at recombination genes is connected to the evolution of recombination rate, we used Coevol, a Bayesian MCMC method that estimates correlations between quantitative traits and substitution rates in a phylogenetic context (Lartillot and Poujol 2010). As a surrogate for recombination rate, we used published estimates of the average number of *MLH1* foci per cell for nine species of mammals: *Homo sapiens, Macaca mulatta, Mus musculus, Rattus norvegicus, Bos taurus, Ovis aries, Equus caballus, Sus scrofa,* and *Canis lupus* (Table S7). To account for variation in karyotypes among species, we divided *MLH1* counts by the number of chromosome arms (autosomal fundamental number [aFN]). Evolutionary correlations between this adjusted recombination rate and substitution rates for each gene were estimated by Coevol 1.5 (Lartillot and Poujol 2010). *RNF212B* was excluded from this analysis due to the lack of sequence data in *R. norvegicus*.

Each analysis was run in duplicate to assess convergence. We report the estimated pairwise correlation coefficients between recombination rate, ω, and *dS*, as well as the partial correlation coefficients for each pairwise correlation (burn-in = 1,000; MCMC chain = 25,000; relative difference $\omega < 0.01$).

Results

RECOMBINATION GENES EVOLVE AT DIFFERENT RATES IN MAMMALS

We used PAML (Yang 1997, 2007) to measure the rate of evolution across the mammalian phylogeny of 32 recombination genes carefully selected to (1) cover each major step in the recombination pathway as evenly as possible, (2) contain genes that have integral functions in each step, and (3) include genes that have been associated with interindividual differences in recombination rate within mammalian populations (Tables 1 and 2).

We observed variation in the rate of evolution of recombination genes, with ω spanning a range of 0.0268 0.8483 (mean ω= 0.3275, SD = 0.1971, median = 0.3095) (Figs. 2 and 3, Table 3). Four genes exhibit particularly rapid evolution when compared to other recombination genes, with evolutionary rates greater than 1SD above the mean (*IHO1, SHOC1, SYCP2, TEX11*). At the other end of the spectrum, five genes have evolutionary rates more than 1SD below the mean and are highly conserved across the mammalian phylogeny (*BRCC3, DMC1, HEI10, RAD50, RAD51*).

In general, there is very high concordance between evolutionary rate across mammals and pairwise divergence between human and macaque (mean ω= 0.3301, SD = 0.2370, median = 0.30925) (Spearman's ρ= 0.833774, $P = 3.11 \times 10^{-9}$) (Fig. 2, Table 4, Fig. S1). The genes that show the most rapid and most conserved rates of divergence between human and macaque are mostly the same genes that show extreme evolutionary rates across the mammalian phylogeny. Notable exceptions include *MEI4* ($\omega_{mammals} = 0.4332$, $\omega_{human-macaque} = 0.7252$), *CNTD1* ($\omega_{mammals} = 0.2496$, $\omega_{human-macaque} = 0.6803$), *HEI10* ($\omega_{mammals} = 0.1226$, $\omega_{human-macaque} = 0.3235$), and *HORMAD1* ($\omega_{mammals} = 0.3036$, $\omega_{human-macaque} = 0.0901$). It should be noted that these two measures are not independent because divergence between human and macaque sequences was incorporated in the phylogenetic analysis across mammals.

RECOMBINATION GENES DISPLAY SIGNATURES OF POSITIVE SELECTION ACROSS MAMMALS

We identified signatures of positive selection in 11 of 32 (34.3%) recombination genes using site models in CODEML: *IHO1, MSH4, MRE11, NBS1, RAD21L, REC8, RNF212, SHOC1, SYCP1, SYCP2,* and *TEX11*. For each of these genes, models that include a fraction of sites where the rate of nonsynonymous substitutions is estimated to be greater than the rate of synonymous substitutions (ω > 1, Model 8) fit better than models that do not include such a class of sites (Model 7, 8a) (Table 2). To mitigate the potential for MNMs to produce false signatures of positive selection, we reanalyzed this subset of genes after removing any codons inferred to have accumulated multiple changes on a single branch (CMDs). After conservatively removing all CMDs, one gene (*TEX11*) retained a significant signature of positive selection (Table 5).

Comparing polymorphism within humans to divergence between human and macaque revealed that 17 of 31 genes depart from neutral predictions in the form of significant McDonald–Kreitman tests (Fisher's exact test, $P < 0.05$; Table 4) (McDonald and Kreitman 1991). These 17 genes harbor an excess of nonsynonymous polymorphisms (Table 4). This

pattern suggests the presence of weakly deleterious mutations at recombination genes in human populations. Contrary to predictions under this model, however, we detected no significant differences in allele frequency between nonsynonymous and synonymous polymorphisms (Wilcoxon rank sum test; $P > 0.05$). None of the recombination genes we surveyed displays a significant excess of nonsynonymous substitutions, the expected signature of positive selection. Only one gene (*TEX11*) has a higher ratio of nonsynonymous to synonymous substitutions than nonsynonymous to synonymous polymorphisms ($NI = 0.7879$; $DoS = 0.0534$) (Table 4).

RECOMBINATION GENE EVOLUTION DEPENDS ON POSITION IN THE PATHWAY AND RECOMBINATION GENES EVOLVE FASTER

To test the hypothesis that genes involved in the crossover/non-crossover decision are more likely to exhibit signatures of rapid and adaptive evolution than genes involved in other aspects of the recombination pathway, we compared the rate of evolution and proportion of positively selected genes between pathway steps. The proportion of genes exhibiting signatures of positive selection varied significantly between steps (Fisher's exact test, $P = 0.0126$). To determine which steps exhibited a significant elevation in the proportion of genes with signatures of positive selection, we ran post hoc analyses comparing each individual step to the rest of the pathway. Although the results were suggestive, after corrections for multiple testing, none of the steps exhibited significant elevations in the proportion of positively selected genes (Table 6). To identify evolutionary patterns that span individual steps, we compared the frequency of positively selected genes among contiguous steps to the rest of the pathway. Significantly more genes involved in synapsis and the crosssover/non-crossover decision exhibit signatures of positive selection across the mammalian phylogeny than genes in the other steps of the recombination pathway (8/11 vs. 3/21, Fisher's exact test, $P = 0.00179$). This result remains significant when applying a Bonferroni correction for multiple testing (11 tests, threshold: $P = 0.0045$).

Comparisons among groups of genes assigned to six major steps in the recombination pathway yielded no significant differences in evolutionary rate (mammals: $P = 0.1422$, Kruskal–Wallis test; human vs. macaque: $P = 0.2682$, Kruskal– Wallis test) (Fig. 4). Similarly, genes acting before and after synapsis show similar evolutionary rates across mammals (average $\omega_{before} = 0.2723$ vs. $\omega_{after} = 0.3762$, $P = 0.1425$, Mann–Whitney U test). Postsynapsis genes show a trend of evolving faster than presynapsis genes in comparisons between human and macaque (average $\omega_{before} = 0.2514$ vs. $\omega_{after} = 0.3994$, $P = 0.05827$, Mann–Whitney U test).

Gradnigo et al. (2016) measured the rate of divergence between human and macaque for 3,606 genes throughout the genome. We used this dataset to ask whether the rate of evolution of recombination genes as a group is different than expected from the genome-wide distribution. Mean rates for sets of 32 ω values randomly sampled from the 3,606-gene list rarely exceeded the mean rate for recombination genes ($P = 0.0075$, 10,000 random draws) (Fig. 5), suggesting that recombination genes evolve faster on average, at least between human and macaque.

RECOMBINATION GENES ASSOCIATED WITH INTERINDIVIDUAL DIFFERENCES DO NOT DIVERGE MORE RAPIDLY BETWEEN SPECIES

Recombination genes previously associated with interindividual differences in recombination rate within species do not evolve significantly faster between species of mammals (average ω= 0.3943 vs. average ω= 0.2925, respectively; $P = 0.2381$, Mann–Whitney U test), although the difference in evolutionary rates between these two classes of genes is greater when considering only divergence between human and macaque (average ω= 0.4181 vs. average ω= 0.2839, respectively; $P = 0.08816$, Mann–Whitney U test). Likewise, the proportion of recombination genes that exhibit signatures of positive selection is not significantly higher among genes that have been associated with interindividual differences (5/11 vs. 6/21; $P = 0.4424$, Fisher's exact test).

EVOLUTIONARY RATES ARE CORRELATED AMONG RECOMBINATION GENES

We used a publicly available database (https://csb.pitt.edu/erc_analysis/index.php) to measure correlations in evolutionary rate among pairs of recombination genes across mammals (Clark et al. 2012). Recombination genes show levels of ERC (mean ERC = 0.134) that are significantly higher than the genome-wide distribution of gene pairs (permutation $P = 0.000358$).

Motivated by the findings that *TEX11, SYCP2,* and *SHOC1* are three of the most rapidly evolving recombination genes among mammals (Table 3) and that *TEX11* has direct protein-to-protein interactions with both *SHOC1* and *SYCP2* (Yang et al. 2008; Guiraldelli et al. 2018), we focused on rate correlations between these genes. *TEX11, SYCP2,* and *SHOC1* show significantly higher rate correlations (mean ERC = 0.42369) than randomly sampled subsets of recombination genes (permutation $P = 0.025$).

THE RATE OF EVOLUTION OF *TEX11* IS POSITIVELY CORRELATED WITH RECOMBINATION RATE IN MAMMALS

To ask whether divergence at recombination genes was connected to the evolution of recombination rate, we used Coevol (Lartillot and Poujol 2010) to detect covariation in these two traits across mammals (Table 7). We used the average number of *MLH1* foci per chromosome arm as an estimate of the genome-wide recombination rate.

One gene, *TEX11*, shows a positive correlation between ω and recombination rate (partial correlation coefficient = 0.756, posterior probability = 0.96) (Fig. 6). Although the statistical significance of these correlations is modest (reflecting the low power of analyses restricted to nine species), these results suggest that *TEX11* evolves faster at the protein level in species with higher rates of recombination. The correlation persists when *MLH1* count per autosomal haploid chromosome number is used (Table S8).

Discussion

Species of mammals recombine at different rates (Burt and Bell 1987; Dumont and Payseur 2008; Smukowski and Noor 2011; Segura et al. 2013; Stapley et al. 2017). The genetic changes responsible for this evolution remain unknown, but they must have occurred in the

pathway that regulates the formation of crossovers. Evaluated in the context of the recombination pathway, our portrait of divergence points to processes and genes that are good candidates for the evolution of recombination rate and shed light 00on the role of natural selection.

Consideration of recombination genes as a group reveals evolutionary patterns. First, the evolutionary rates of recombination genes are correlated across the mammalian phylogeny. This result is consistent with a broader pattern of ERC among meiosis genes (Clark et al. 2013), as well as the hypothesis that functionally interacting genes experience concordant evolutionary pressures (Clark et al. 2012, 2013; Priedigkeit et al. 2015). Second, recombination genes tend to evolve faster than other genes, at least based on comparisons between human and macaque. There are multiple features of recombination genes that could generate this pattern. The restriction of expression of some recombination genes to meiotic cells could reduce the pleiotropic consequences of amino acid substitutions (Duret and Mouchiroud 1999; Liao et al. 2006). Additionally, the central role of recombination genes in reproduction could accelerate their divergence (Swanson and Vacquier 2002; Dapper and Wade 2016). A third possibility is that recombination itself is frequently subject to directional selection (Segura et al. 2013; Dapper and Payseur 2017; Ritz et al. 2017), driving divergence at the underlying genes.

Eleven of the 32 recombination genes we examined display signatures of positive selection across the mammalian phylogeny. If directional selection has driven the evolution of recombination rate in mammals (Segura et al. 2013), we would expect signatures of positive selection to be localized near the crossover/non-crossover decision point in the pathway. In support of this prediction, 8 of the 11 genes with evidence for adaptive evolution act primarily to form the SC (*REC8, RAD21L, SYCP1,* and *SYCP2*; Parisi et al. 1999; de Vries et al. 2005; Yang et al. 2006; Lee and Hirano 2011) and to regulate the first steps of the crossover versus non-crossover decision (*TEX11, SHOC1, RNF212,* and *MSH4*; Snowden et al. 2004; Yang et al. 2008; Qiao et al. 2014; Guiraldelli et al. 2018). Further evidence of a role for directional selection (to increase recombination) comes from the positive correlation between divergence at the most rapidly evolving recombination gene (*TEX11*) and the genome-wide recombination rate, although the posterior probability of this correlation is modest (in light of multiple testing). The inference of recurrent directional selection on genes that function during meiosis also raises the possibility that divergence could be connected to genetic conflict. For example, theoretical work suggests that recombination rate can evolve to suppress meiotic drive (Brandvain and Coop 2012).

Deeper consideration of evolution at *TEX11* provides additional insights about the connection between molecular evolution and recombination rate evolution. Fourteen amino acid residues in *TEX11* exhibit patterns consistent with adaptive evolution (BEB, $P > 0.95$). In contrast to *MSH4* or *PRDM9*, where targets of selection localize to certain protein domains (Oliver et al. 2009; Thomas et al. 2009; Grey et al. 2011) the *TEX11* residues of interest are distributed across the length of the gene. This pattern matches aspects of *TEX11* protein function. The gene encompasses three large, ubiquitous protein interaction (TRP) domains (Guiraldelli et al. 2018). Most of the residues with signatures of selection localize to two of the large TRP domains, one of which is known to bind to *SHOC1* (Guiraldelli et

al. 2018). The putative function of *TEX11* is to bind to the SC (i.e., *SYCP2*) and recruit proteins that designate which DSBs become crossovers (i.e., *SHOC1*), a pivotal role at the early stages of the crossover versus non-crossover decision (Guiraldelli et al. 2018). The rates of molecular evolution of *TEX11, SYCP2,* and *SHOC1* are significantly more correlated with each other than expected given observed correlations among all surveyed recombination genes. Additionally, these three genes (along with *IHO1*) exhibit the highest rates of evolution across the mammalian phylogeny. Mutations in *TEX11* are associated with differences in recombination rate in humans and in transgenic mice (Yang et al. 2015). *TEX11* is also a candidate gene for a quantitative trait locus that contributes to variation in recombination rate among inbred mouse strains (Murdoch et al. 2010). Although *TEX11* is named for a pattern of testes-specific expression, it affects recombination in females as well as males (Yang et al. 2015).

Five of the genes that exhibit signatures of positive selection across the mammalian phylogeny have been associated with interindividual variation in recombination rate within species: *RAD21L* (Kong et al. 2014), *REC8* (Sandor et al. 2012; Johnston et al. 2016, 2018), *MSH4* (Kong et al. 2014; Ma et al. 2015; Kadri et al. 2016; Shen et al. 2018), *RNF212* (Kong et al. 2008; Chowdhury et al. 2009; Fledel-Alon et al. 2011; Sandor et al. 2012; Johnston et al. 2016; Kadri et al. 2016; Petit et al. 2017), and *TEX11* (Murdoch et al. 2010). However, as a group, recombination genes previously associated with intraspecific variation in the genome-wide recombination rate evolve at similar rates to recombination genes lacking such an association. Two factors are likely to weaken the association between genes that contribute to differences within species and those that diverge most rapidly between species. First, genes responsible for species differences in recombination rate could be subject to strong directional selection within populations, reducing their contributions to intraspecific variation. Second, genes that confer within-species rate variation could be targets of diversifying or antagonistic selection, limiting their divergence between species. For example, variants at *RNF212*, a gene associated with intraspecific variation in recombination rate in several mammalian species, have contrasting effects in women and men (Kong et al. 2008).

The structure of genetic pathways is expected to influence evolutionary trajectories (Rausher et al. 1999; Lu and Rausher 2003). Matching this prediction, recombination genes show relatively high rate correlations compared to other sets of genes. Nevertheless, our results suggest that the selection pressures targeting a gene are not easily deduced from its position in the recombination pathway. Perhaps rate variation among domains within proteins masks a clearer effect of pathway position. For example, the signal of adaptive evolution in *PRDM9* is restricted to the zinc finger residues, with much of the gene sequence being conserved between species (Oliver et al. 2009; Thomas et al. 2009). Rate heterogeneity between genes within steps of the recombination pathway motivates a more thorough investigation of functional domains in genes of interest.

Despite evidence for positive selection across the mammalian phylogeny, comparisons of polymorphism and divergence yielded no significant signatures of adaptive evolution between human and macaque. Instead, many recombination genes display an excess of nonsynonymous polymorphisms, consistent with an accumulation of weakly deleterious

mutations within humans. This approach searches for patterns of selection at the level of the entire gene, whereas positive selection can target certain domains. For example, *MSH4* exhibits evidence for adaptive evolution along the mammalian phylogeny and shows an excess of nonsynonymous polymorphisms within humans. These two seemingly disparate results are unified by the observation that all six codons in *MSH4* with significant signatures of positive selection (BEB, $P > 0.95$) are highly localized in the first 100-bp of the gene, in a putative DNA binding domain (Rakshambikai et al. 2013; Piovesan et al. 2017).

Our results highlight an evolutionary contrast between mammals and Drosophila. *MCMDC2*, the mammalian homolog of the *mei-217/mei-218* gene that evolves rapidly and adaptively in Drosophila (Brand et al. 2018), exhibits below-average rates of evolution compared to other recombination genes and shows no evidence of positive selection. These two homologs occupy different positions in the recombination pathway. In Drosophila, *mei-218* has evolved to replace the function of the missing *MSH4* and *MSH5* (Kohl et al. 2012; Finsterbusch et al.2016). This shift in both evolutionary rate and pathway function suggests that functional homology is a better predictor of evolutionary rate than sequence homology for this recombination gene. Conversely, no ortholog of *TEX11* has yet been identified in Drosophila. How-ever, meiosis-specific orthologs of *TEX11* (Zip4) are present in the yeast (*Saccharomyces cerevisiae*) and Arabidopsis (*Arabidopsis thaliana*) genomes (Adelman and Petrini 2008), motivating investigation into the deeper evolutionary history of *TEX11*.

One cost of the increased sensitivity of PAML is an inflation of the false-positive rate in the presence of multinucleotide substitutions (Venkat et al. 2018). It was not possible to directly identify MNMs in our dataset, so we chose the highly conservative approach of removing all codons inferred to have accumulated multiple mutations on a single branch in the phylogeny. Codons removed using this approach could be MNMs, but they also likely include codons that either have accumulated sequential mutations along the long branches in the mammalian phylogeny or are neither MNMs nor CMDs, due to uncertainty in the inference of ancestral sequences. Despite the conservative nature of this approach, we still found a signature of positive selection in *TEX11*, even when all putative CMDs were removed. Nevertheless, differences in the results with and without filtering make it difficult to draw conclusions about the robustness of signals of selection in the other recombination genes.

Sex differences in recombination rate, known as heterochi-asmy, are widespread in mammals (Burt et al. 1991; Lenormand and Dutheil 2005). We used only testes expression datasets to identify the relevant isoform of each gene because fetal ovary expression datasets were not available. It is conceivable that the isoforms of these genes are sexually dimorphic. Additionally, estimates of the genome-wide recombination rate from *MLH1* counts were not available for females in most of the species we surveyed. Due to these biases in existing datasets, our analyses could have missed female-specific evolutionary dynamics of the recombination pathway.

Another caveat concerns the interpretation of our findings. Although we would prioritize rapidly evolving genes with evidence of adaptive evolution as candidates, evolution of the recombination rate between species could be caused by only a few amino acid substitutions

(especially along particular mammalian lineages) or by regulatory changes located outside protein-coding regions or in transcription factors. We also cannot preclude the existence of undiscovered genetic, epigenetic, or environmental modifiers of recombination rate. We hope our results will motivate genetic dissection of between-species differences in recombination rate through functional evaluation of the candidate genes we identified, especially *TEX11* and associated genes involved in the SC and early stages of the crossover/non-crossover decision.

Supplementary Material

Refer to Web version on PubMed Central for supplementary material.

ACKNOWLEDGMENTS

We thank Nathan Clark for assistance with evolutionary covariation rate analyses and Francesca Cole for advice on selection of recombination genes. A.L.D. was supported by NHGRI Training Grant to the Genomic Sciences Training Program 5T32HG002760. B.A.P. was supported by NIH grant R01 GM120051.

LITERATURE CITED

Abascal F, Zardoya R, and Telford MJ. 2010 Translatorx: multiple alignment of nucleotide sequences guided by amino acid translations. Nucleic Acids Res. 38(Suppl. 2):W7–W13. [PubMed: 20435676]

Adelman CA, and Petrini JH. 2008 Zip4h (tex11) deficiency in the mouse impairs meiotic double strand break repair and the regulation of crossing over. PLoS Genet. 4:e1000042.

Baker SM, Plug AW, Prolla TA, Bronner CE, Harris AC, Yao X, Christie D-M, Monell C, Arnheim N, Bradley A, et al. 1996 Involvement of mouse Mlh1 in DNA mismatch repair and meiotic crossing over. Nat. Gen 13:336.

Balcova M, Faltusova B, Gergelits V, Bhattacharyya T, Mihola O, Trachtulec Z, Knopf C, Fotopulosova V, Chvatalova I, Gregorova S, et al. 2016 Hybrid sterility locus on chromosome X controls meiotic recombination rate in mouse. PLoS Genet. 12:e1005906.

Barbosa-Morais NL, Irimia M, Pan Q, Xiong HY, Gueroussov S, Lee LJ, Slobodeniuc V, Kutter C, Watt S, Çolak R, et al. 2012 The evolutionary landscape of alternative splicing in vertebrate species. Science 338:1587–1593. [PubMed: 23258890]

Barrett T, Wilhite SE, Ledoux P, Evangelista C, Kim IF, Toma-shevsky M, Marshall KA, Phillippy KH, Sherman PM, Holko M, et al. 2012 NCBI geo: archive for functional genomics data sets–update. Nucleic Acids Res. 41(D1):D991–D995. [PubMed: 23193258]

Baudat F, and de Massy B. 2007 Regulating double-stranded DNA break repair towards crossover or non-crossover during mammalian meiosis. Chromosome Res. 15:565–577. [PubMed: 17674146]

Baudat F, Manova K, Yuen JP, Jasin M, and Keeney S. 2000Chromosome synapsis defects and sexually dimorphic meiotic progression in mice lacking Spo11. Mol. Cell 6:989–998. [PubMed: 11106739]

Begun DJ, and Aquadro CF. 1992 Levels of naturally occurring DNA polymorphism correlate with recombination rates in D. melanogaster. Nature 356:519. [PubMed: 1560824]

Bergerat A, de Massy B, Gadelle D, Varoutas P-C, Nicolas A, and Forterre P. 1997 An atypical topoisomerase II from Archaea with implications for meiotic recombination. Nature 386:414. [PubMed: 9121560]

Besenbacher S, Sulem P, Helgason A, Helgason H, Kristjansson H, Jonasdottir A, Jonasdottir A, Magnusson OT, Thorsteinsdottir U, Masson G, et al. 2016 Multi-nucleotide de novo mutations in humans.PLoS Genet. 12:e1006315.

Bisig CG, Guiraldelli MF, Kouznetsova A, Scherthan H, Höög C, Dawson DS, and Pezza RJ. 2012Synaptonemal complex components persist at centromeres and are required for homologous centromere pairing in mouse spermatocytes. PLoS Genet. 8:e1002701.

Bolcun-Filas E, and Schimenti JC. 2012 Genetics of meiosis and recombination in mice. Int. Rev. Cell Mol. Biol 298:179–227.

Brand CL, Cattani MV, Kingan SB, Landeen EL, and Presgraves DC. 2018 Molecular evolution at a meiosis gene mediates species differences in the rate and patterning of recombination. Curr. Biol 28:1289–1295. [PubMed: 29606420]

Brandvain Y, and Coop G. 2012 Scrambling eggs: meiotic drive and the evolution of female recombination rates. Genetics 190:709–723. [PubMed: 22143919]

Broman KW, Murray JC, Sheffield VC, White RL, and Weber JL. 1998 Comprehensive human genetic maps: individual and sex-specific variation in recombination. Am. J. Hum. Genet 63:861–869. [PubMed: 9718341]

Brown MS, and Bishop DK. 2014 DNA strand exchange and RecA homologs in meiosis. Cold Spring Harb. Perspect. Biol 2014:a016659.

Burt A, and Bell G. 1987 Red queen versus tangled bank models. Nature 330:118.

Burt A, Bell G, and Harvey PH. 1991 Sex differences in recombination. J. Evol. Biol 4:259–277.

Charlesworth B, Morgan M, and Charlesworth D. 1993 The effect of deleterious mutations on neutral molecular variation. Genetics 134:1289–1303. [PubMed: 8375663]

Charlesworth B, Jarne P, and Assimacopoulos S. 1994 The distribution of transposable elements within and between chromosomes in a population of Drosophila melanogaster. III. Element abundances in heterochromatin. Gen. Res 64:183–197.

Chen M-Y, Liang D, and Zhang P. 2017 Phylogenomic resolution of the phylogeny of Laurasiatherian mammals: exploring phylogenetic signals within coding and noncoding sequences. Genome Biol. Evol 9:1998–2012. [PubMed: 28830116]

Chowdhury R, Bois PR, Feingold E, Sherman SL, and Cheung VG. 2009 Genetic analysis of variation in human meiotic recombination. PLoS Genet. 5:e1000648.

Clark NL, Gasper J, Sekino M, Springer SA, Aquadro CF, and Swanson WJ. 2009 Coevolution of interacting fertilization proteins. PLoS Genet. 5:e1000570.

Clark NL, Alani E, and Aquadro CF. 2012 Evolutionary rate covariation reveals shared functionality and coexpression of genes. Genome Res.22:714–720. [PubMed: 22287101]

Clark NL, Alani E, and Aquadro CF. 2013 Evolutionary rate covariation in meiotic proteins results from fluctuating evolutionary pressure in yeasts and mammals. Genetics 193:529–538. [PubMed: 23183665]

Cloud V, Chan Y-L, Grubb J, Budke B, and Bishop DK. 2012 Rad51 is anaccessoryfactorforDMC1-mediatedjointmoleculeformationduring meiosis. Science 337:1222–1225. [PubMed: 22955832]

Cole F, Kauppi L, Lange J, Roig I, Wang R, Keeney S, and Jasin M. 2012 Homeostatic control of recombination is implemented progressively in mouse meiosis. Nature cell biology 14:424. [PubMed: 22388890]

Comeron JM, Kreitman M, and Aguadé M. 1999 Natural selection oń synonymous sites is correlated with gene length and recombination in drosophila. Genetics 151:239–249. [PubMed: 9872963]

Comeron JM, Ratnappan R, and Bailin S. 2012 The many landscapes of recombination in Drosophila melanogaster. PLoS Genet. 8:e1002905.

Coop G, and Przeworski M. 2007 An evolutionary view of human recombination. Nat. Rev. Genet 8:23. [PubMed: 17146469]

Costa Y, Speed R, Öllinger R, Alsheimer M, Semple CA, Gautier P, Maratou K, Novak I, Höög C, Benavente R, et al. 2005 Two novel proteins recruited by synaptonemal complex protein 1 (SYCP1) are at the centre of meiosis. J. Cell Sci 118:2755–2762. [PubMed: 15944401]

Dapper AL, and Payseur BA. 2017 Connecting theory and data to understand recombination rate evolution. Philos. Trans. R. Soc. B 372:20160469.

Dapper AL, and Wade MJ. 2016 The evolution of sperm competition genes: the effect of mating system on levels of genetic variation within and between species. Evolution 70:502–511. [PubMed: 26748568]

de Vries FA, de Boer E, van den Bosch M, Baarends WM, Ooms M, Yuan L, Liu J-G, van Zeeland AA, Heyting C, and Pastink A. 2005 Mouse sycp1 functions in synaptonemal complex assembly, meiotic recombination, and xy body formation. Genes Dev. 19:1376–1389. [PubMed: 15937223]

de Vries SS, Baart EB, Dekker M, Siezen A, de Rooij DG, de Boer P, and te Riele H. 1999 Mouse MutS-like protein Msh5 is required for proper chromosome synapsis in male and female meiosis. Genes Dev. 13:523–531. [PubMed: 10072381]

Dumont BL, and Payseur BA. 2008 Evolution of the genomic rate of recombination in mammals. Evolution 62:276–294. [PubMed: 18067567]

Dumont BL, and Payseur BA. 2011 Genetic analysis of genome-scale recombination rate evolution in house mice. PLoS Genet. 7:e1002116.

Dumont BL, White MA, Steffy B, Wiltshire T, and Payseur BA. 2011 Extensive recombination rate variation in the house mouse species complex inferred from genetic linkage maps. Genome Res. 21:114–125. [PubMed: 20978138]

Duret L, and Arndt PF. 2008 The impact of recombination on nucleotide substitutions in the human genome. PLoS Genet. 4:e1000071.

Duret L, and Mouchiroud D. 1999 Expression pattern and, surprisingly, gene length shape codon usage in Caenorhabditis, Drosophila, and Arabidopsis. Proc. Natl. Acad. Sci 96:4482–4487. [PubMed: 10200288]

Edelmann W,Cohen PE, Kane M, Lau K, Morrow B, Bennett S, Umar A, Kunkel T, Cattoretti G, Chaganti R, et al. 1996 Meiotic pachytene arrest in MLH1-deficient mice. Cell 85:1125–1134. [PubMed: 8674118]

Edgar RC 2004 Muscle: multiple sequence alignment with high accuracy and high throughput. Nucleic Acids Res. 32:1792–1797. [PubMed: 15034147]

Fan Y, Huang Z-Y, Cao C-C, Chen C-S, Chen Y-X, Fan D-D, He J, Hou H-L, Hu L, Hu X-T, et al. 2013 Genome of the Chinese tree shrew. Nat. Commun 4:1426. [PubMed: 23385571]

Fay JC, Wyckoff GJ, and Wu C-I. 2001 Positive and negative selection on the human genome. Genetics 158:1227–1234. [PubMed: 11454770]

Felsenstein J 1974 The evolutionary advantage of recombination. Genetics 78:737–756. [PubMed: 4448362]

Finsterbusch F, Ravindranathan R, Dereli I, Stanzione M, Tränkner D, and Tóth A. 2016 Alignment of homologous chromosomes and effective repair of programmed dna double-strand breaks during mouse meiosis require the minichromosome maintenance domain containing 2 (MCMDC2) protein. PLoS Genet. 12:e1006393.

Fledel-Alon A, Leffler EM, Guan Y, Stephens M, Coop G, and Przeworski M. 2011 Variation in human recombination rates and its genetic determinants. PloS One 6:e20321.

Fraune J, Alsheimer M, Redolfi J, Brochier-Armanet C, and Benavente R. 2014 Protein SYCP2 is an ancient component of the metazoan synaptonemal complex. Cytogenet. Genome Res 144:299–305. [PubMed: 25831978]

Fukuda T, Daniel K, Wojtasz L, Toth A, and Höög C. 2010 A novel mammalian horma domain-containing protein, hormad1, preferentially associates with unsynapsed meiotic chromosomes. Exp. Cell Res 316:158–171. [PubMed: 19686734]

Gonen S, Battagin M, Johnston SE, Gorjanc G, and Hickey JM. 2017 The potential of shifting recombination hotspots to increase genetic gain in livestock breeding. Genet. Select. Evol 49:55.

Gradnigo JS, Majumdar A, Norgren RB Jr, and Moriyama EN. 2016 Advantages of an improved rhesus macaque genome for evolutionary analyses. PloS One 11:e0167376.

Grey C, Barthès P, Chauveau-Le Friec G, Langa F, Baudat F, and dè Massy B. 2011 Mouse PRDM9 DNA-binding specificity determines sites of histone H3 lysine 4 trimethylation for initiation of meiotic recombination. PLoS Biol. 9:e1001176.

Guiraldelli MF, Eyster C, Wilkerson JL, Dresser ME, and Pezza RJ. 2013 Mouse HFM1/Mer3 is required for crossover formation and complete synapsis of homologous chromosomes during meiosis. PLoS Genet. 9:e1003383.

Guiraldelli MF, Felberg A, Almeida LP, Parikh A, de Castro RO, and Pezza RJ. 2018 Shoc1 is a ERCC4-(HhH) 2-like protein, integral to the formation of crossover recombination intermediates during mammalian meiosis. PLoS Genet. 14:e1007381.

Hakes L, Lovell SC, Oliver SG, and Robertson DL. 2007 Specificity in protein interactions and its relationship with sequence diversity and coevolution. Proc. Nat Acad. Sci 104:7999–8004. [PubMed: 17468399]

Hamer G, Gell K, Kouznetsova A, Novak I, Benavente R, and Höög C. 2006 Characterization of a novel meiosis-specific protein within the central element of the synaptonemal complex. J. Cell Sci 119:4025–4032. [PubMed: 16968740]

Hamer G, Wang H, Bolcun-Filas E, Cooke HJ, Benavente R, and Höög C. 2008 Progression of meiotic recombination requires structural maturation of the central element of the synaptonemal complex. J. Cell Sci 121:2445–2451. [PubMed: 18611960]

Hassold T, and Hunt P. 2001 To err (meiotically) is human: the genesis of human aneuploidy. Nat. Rev. Genet 2:280. [PubMed: 11283700]

Hernández-Hernández A, Masich S, Fukuda T, Kouznetsova A, Sandin S, Daneholt B, and Höög C. 2016 The central element of the synaptonemal complex in mice is organized as a bilayered junction structure. J. Cell Sci 129:2239–2249. [PubMed: 27103161]

Hill WG, and Robertson A. 1966 The effect of linkage on limits to artificial selection. Genet. Res 8:269–294. [PubMed: 5980116]

Holloway JK, Booth J, Edelmann W, McGowan CH, and Cohen PE. 2008 Mus81 generates a subset of mlh1-mlh3–independent crossovers in mammalian meiosis. PLoS Genet. 4:e1000186.

Holloway JK, Sun X, Yokoo R, Villeneuve AM, and Cohen PE. 2014 Mammalian cntd1 is critical for meiotic crossover maturation and deselection of excess precrossover sites. J. Cell Biol 205:633–641. [PubMed: 24891606]

Hunter CM, Huang W, Mackay TF, and Singh ND. 2016 The genetic architecture of natural variation in recombination rate in Drosophila melanogaster. PLoS Genet. 12:e1005951.

Jeffreys AJ, Neumann R, Panayi M, Myers S, and Donnelly P. 2005 Human recombination hot spots hidden in regions of strong marker association. Nat. Genet 37:601. [PubMed: 15880103]

Johnston SE, Bérénos C, Slate J, and Pemberton JM. 2016 Conserved´ genetic architecture underlying individual recombination rate variation in a wild population of Soay sheep (Ovis aries). Genetics 203:583–598. [PubMed: 27029733]

Johnston SE, Huisman J, and Pemberton JM. 2018 A genomic region containing REC8 and RNF212B is associated with individual recombination rate variation in a wild population of red deer (Cervus elaphus). G3 8:2265–2276. [PubMed: 29764960]

Kadri NK, Harland C, Faux P, Cambisano N, Karim L, Coppieters W, Fritz S, Mullaart E, Baurain D, Boichard D, et al. 2016 Coding and noncoding variants in HFM1, MLH3, MSH4, MSH5, RNF212, and RNF212B affect recombination rate in cattle. Genome Res. 26:1323–1332. [PubMed: 27516620]

Keeney S 2007 Spo11 and the formation of DNA double-strand breaks in meiosis. Genome Dyn. Stab 2:81–123.

Keeney S, Giroux CN, and Kleckner N. 1997 Meiosis-specific DNA double-strand breaks are catalyzed by Spo11, a member of a widely conserved protein family. Cell 88:375–384. [PubMed: 9039264]

Kobayashi W, Takaku M, Machida S, Tachiwana H, Maehara K, Ohkawa Y, and Kurumizaka H. 2016 Chromatin architecture may dictate the target site for DMC1, but not for RAD51, during homologous pairing. Sci. Rep 6:24228.

Kohl KP, Jones CD, and Sekelsky J. 2012 Evolution of an MCM complex in flies that promotes meiotic crossovers by blocking BLM helicase. Science 338:1363–1365. [PubMed: 23224558]

Kong A, Thorleifsson G, Stefansson H, Masson G, Helgason A, Gudbjartsson DF, Jonsdottir GM, Gudjonsson SA, Sverrisson S, Thorlacius T, et al. 2008 Sequence variants in the RNF212 gene associate with genome-wide recombination rate. Science 319:1398–1401. [PubMed: 18239089]

Kong A, Thorleifsson G, Gudbjartsson DF, Masson G, Sigurdsson A, Jonasdottir A,Walters GB,Jonasdottir A,Gylfason A,Kristinsson KT, et al. 2010 Fine-scale recombination rate differences between sexes, populations and individuals. Nature 467:1099. [PubMed: 20981099]

Kong A, Thorleifsson G, Frigge ML, Masson G, Gudbjartsson DF, Villemoes R, Magnusdottir E, Olafsdottir SB, Thorsteinsdottir U, and Stefansson K. 2014 Common and low-frequency variants associated with genome-wide recombination rate. Nat. Genet 46:11. [PubMed: 24270358]

Kumar R, Bourbon H-M, and de Massy B. 2010 Functional conservation of mei4 for meiotic dna double-strand break formation from yeasts to mice. Genes Dev. 24:1266–1280. [PubMed: 20551173]

Kumar R, Ghyselinck N, Ishiguro K-I, Watanabe Y, Kouznetsova A, Höög C, Strong E, Schimenti J, Daniel K, Toth A, et al. 2015 MEI4: a central player in the regulation of meiotic DNA double strand break formation in the mouse. J. Cell Sci 128:1800–1811. [PubMed: 25795304]

Kumar R, Oliver C, Brun C, Juarez-Martinez AB, Tarabay Y, Kadlec J, and de Massy B. 2018 Mouse REC114 is essential for meiotic DNA double-strand break formation and forms a complex with MEI4. Life Sci. Alliance 1:e201800259.

La Salle S, Palmer K, O'Brien M, Schimenti JC, Eppig J, and Handel MA. 2012 Spata22, a novel vertebrate-specific gene, is required for meiotic progress in mouse germ cells. Biol. Reprod 86:45–1. [PubMed: 22011390]

Lamarche BJ, Orazio NI, and Weitzman MD. 2010 The mrn complex in double-strand break repair and telomere maintenance. FEBS Lett.584:3682–3695. [PubMed: 20655309]

Lange J, Yamada S, Tischfield SE, Pan J, Kim S, Zhu X, Socci ND, Jasin M, and Keeney S. 2016 The landscape of mouse meiotic double-strand break formation, processing, and repair. Cell 167:695–708. [PubMed: 27745971]

Langmead B, and Salzberg SL. 2012 Fast gapped-read alignment with Bowtie 2. Nat. Meth 9:357.

Lartillot N, and Poujol R. 2010 A phylogenetic model for investigating correlated evolution of substitution rates and continuous phenotypic characters. Mol. Biol. Evol 28:729–744. [PubMed: 20926596]

Lee J, and Hirano T. 2011 RAD21L, a novel cohesin subunit implicated in linking homologous chromosomes in mammalian meiosis. J. Cell Biol 192:263–276. [PubMed: 21242291]

Leinonen R, Sugawara H, Shumway M, and I. N. S. D. Collaboration. 2010 The sequence read archive. Nucleic Acids Res. 39(Suppl. 1):D19–D21. [PubMed: 21062823]

Lek M, Karczewski KJ, Minikel EV, Samocha KE, Banks E, Fennell T, O'Donnell-Luria AH, Ware JS, Hill AJ, Cummings BB, et al. 2016 Analysis of protein-coding genetic variation in 60,706 humans. Nature 536:285. [PubMed: 27535533]

Lenormand T,and Dutheil J.2005Recombinationdifferencebetweensexes: a role for haploid selection. PLoS Biol. 3:e63.

Letunic I, and Bork P. 2019 Interactive tree of life (iTOL) v4: recent updates and new developments. Nucleic Acids Res. 47:W256–W259. [PubMed: 30931475]

Li H, Handsaker B, Wysoker A, Fennell T, Ruan J, Homer N, Marth G, Abecasis G, and Durbin R. 2009 The sequence alignment/map format and samtools. Bioinformatics 25:2078–2079. [PubMed: 19505943]

Liao B-Y, Scott NM, and Zhang J. 2006 Impacts of gene essentiality, expression pattern, and gene compactness on the evolutionary rate of mammalian proteins. Mol. Biol. Evol 23:2072–2080. [PubMed: 16887903]

Lipkin SM, Moens PB, Wang V, Lenzi M, Shanmugarajah D, Gilgeous A, Thomas J, Cheng J, Touchman JW, Green ED, et al. 2002 Meiotic arrest and aneuploidy in MLH3-deficient mice. Nat. Genet 31:385. [PubMed: 12091911]

Lu Y, and Rausher MD. 2003 Evolutionary rate variation in anthocyanin pathway genes. Mol. Biol. Evol 20:1844–1853. [PubMed: 12885963]

Luo M, Yang F, Leu NA, Landaiche J, Handel MA, Benavente R, La Salle S, and Wang PJ. 2013 MEIOB exhibits single-stranded DNA-binding and exonuclease activities and is essential for meiotic recombination. Nat. Commun 4:2788. [PubMed: 24240703]

Ma L, O'Connell JR, VanRaden PM, Shen B, Padhi A, Sun C, Bickhart DM, Cole JB, Null DJ, Liu GE, et al. 2015 Cattle sex-specific recombination and genetic control from a large pedigree analysis. PLoS Genet. 11:e1005387.

McDonald JH, and Kreitman M. 1991 Adaptive protein evolution at the Adh locus in Drosophila. Nature 351:652. [PubMed: 1904993]

Meuwissen R, Offenberg HH, Dietrich A, Riesewijk A, van Iersel M, and Heyting C. 1992 A coiled-coil related protein specific for synapsed regions of meiotic prophase chromosomes. EMBO J. 11:5091. [PubMed: 1464329]

Murdoch B, Owen N, Shirley S, Crumb S, Broman KW, and Hassold T. 2010 Multiple loci contribute to genome-wide recombination levels in male mice. Mamm. Genome 21:550–555. [PubMed: 21113599]

Myers S, Bowden R, Tumian A, Bontrop RE, Freeman C, MacFie TS, McVean G, and Donnelly P. 2010 Drive against hotspot motifs in primates implicates the prdm9 gene in meiotic recombination. Science 327:876–879. [PubMed: 20044541]

Oh J, Al-Zain A, Cannavo E, Cejka P, and Symington LS. 2016 Xrs2 dependent and independent functions of the Mre11-Rad50 complex. Mol. Cell 64:405–415. [PubMed: 27746018]

Oliver PL, Goodstadt L, Bayes JJ, Birtle Z, Roach KC, Phadnis N, Beatson SA, Lunter G, Malik HS, and Ponting CP. 2009 Accelerated evolution of the Prdm9 speciation gene across diverse metazoan taxa. PLoS Gen. 5:e1000753.

Page SL, and Hawley RS. 2004 The genetics and molecular biology of the synaptonemal complex. Annu. Rev. Cell Dev. Biol 20:525–558. [PubMed: 15473851]

Paigen K, and Petkov PM. 2018 Prdm9 and its role in genetic recombination. Trends Genet. 34:291–300. [PubMed: 29366606]

Pamilo P, and Nei M. 1988 Relationships between gene trees and species trees. Mol. Biol. Evol 5:568–583. [PubMed: 3193878]

Pan Q, Shai O, Lee LJ, Frey BJ, and Blencowe BJ. 2008 Deep surveying of alternative splicing complexity in the human transcriptome by high-throughput sequencing. Nat. Genet 40:1413. [PubMed: 18978789]

Parisi S, McKay MJ, Molnar M, Thompson MA, Van Der Spek PJ, van Drunen-Schoenmaker E, Kanaar R, Lehmann E, Hoeijmakers JH, and Kohli J. 1999 Rec8p, a meiotic recombination and sister chromatid cohesion phosphoprotein of the Rad21p family conserved from fission yeast to humans. Mol. Cell. Biol 19:3515–3528. [PubMed: 10207075]

Parvanov ED, Petkov PM, and Paigen K. 2010 Prdm9 controls activation of mammalian recombination hotspots. Science 327:835–835. [PubMed: 20044538]

Pazos F, and Valencia A. 2001 Similarity of phylogenetic trees as indicator of protein–protein interaction. Protein Eng. 14:609–614. [PubMed: 11707606]

Perelman P, Johnson WE, Roos C, Seuanez HN, Horvath JE, Moreira MA, Kessing B, Pontius J, Roelke M, Rumpler Y, et al. 2011 A molecular phylogeny of living primates. PLoS Genet. 7:e1001342.

Petit M, Astruc J-M, Sarry J, Drouilhet L, Fabre S, Moreno C, and Servin B.2017Variation in recombination rate and its genetic determinism in sheep populations. Genetics 207:767–784. [PubMed: 28978774]

Piovesan D, Tabaro F, Paladin L, Necci M, Mičetić I, Camilloni C, Davey N, Dosztányi Z, Mészáros B, Monzon AM. et al. 2017 Mobidb´ 3.0: more annotations for intrinsic disorder, conformational diversity and interactions in proteins. Nucleic Acids Res. 46(D1):D471–D476.

Prasad AB, Allard MW, Program NCS, and Green ED. 2008 Confirming the phylogeny of mammals by use of large comparative sequence data sets. Mol. Biol. Evol 25:1795–1808. [PubMed: 18453548]

Priedigkeit N, Wolfe N, and Clark NL. 2015 Evolutionary signatures amongst disease genes permit novel methods for gene prioritization and construction of informative gene-based networks. PLoS Genet. 11:e1004967.

Qiao H, Rao HP, Yang Y, Fong JH, Cloutier JM, Deacon DC, Nagel KE, Swartz RK, Strong E, Holloway JK, et al. 2014 Antagonistic roles of ubiquitin ligase HEI10 and SUMO ligase RNF212 regulate meiotic recombination. Nat. Genet 46:194. [PubMed: 24390283]

Rakshambikai R, Srinivasan N, and Nishant KT. 2013 Structural insights into Saccharomyces cerevisiae Msh4–Msh5 complex function using homology modeling. PLoS One 8:e78753.

Rao HP, Qiao H, Bhatt SK, Bailey LR, Tran HD, Bourne SL, Qiu W, Deshpande A, Sharma AN, Beebout CJ, et al. 2017 A sumoubiquitin relay recruits proteasomes to chromosome axes to regulate meiotic recombination. Science 355:403–407. [PubMed: 28059716]

Rausher MD, Miller RE, and Tiffin P. 1999 Patterns of evolutionary rate variation among genes of the anthocyanin biosynthetic pathway. Mol. Biol. Evol 16:266–274. [PubMed: 10028292]

R Core Team. 2015 R: A language and environment for statistical computing. R Foundation for Statistical Computing, Vienna, Austria.

Reynolds A, Qiao H, Yang Y, Chen JK, Jackson N, Biswas K, Holloway JK, Baudat F, de Massy B, Wang J, et al. 2013 Rnf212 is a dosage-sensitive regulator of crossing-over during mammalian meiosis. Nat. Genet 45:269. [PubMed: 23396135]

Ritz KR, Noor MA, and Singh ND. 2017 Variation in recombination rate: adaptive or not? Trends Genet. 33:364–374. [PubMed: 28359582]

Rogacheva MV, Manhart CM, Chen C, Guarne A, Surtees J, and Alani E. 2014 Mlh1-Mlh3, a meiotic crossover and DNA mismatch repair factor, is a Msh2-Msh3-stimulated endonuclease. J. Biol. Chem 289:5664–5673. [PubMed: 24403070]

Romanienko PJ, and Camerini-Otero RD. 2000 The mouse Spo11 gene is required for meiotic chromosome synapsis. Mol. Cell 6:975–987.

Ronquist F,Teslenko M, Van Der Mark P, Ayres DL, Darling A, Höhna S, Larget B, Liu L, Suchard MA, and Huelsenbeck JP. 2012 Mrbayes 3.2: efficient Bayesian phylogenetic inference and model choice across a large model space. Syst. Biol 61:539–542. [PubMed: 22357727]

Rosenberg NA 2002 The probability of topological concordance of gene trees and species trees. Theor. Popul.Biol 61:225–247. [PubMed: 11969392]

Ruiz-Herrera A, Vozdova M, Fernández J, Sebestova H, Capilla L, Frohlich J, Vara C, Hernández-Marsal A, Sipek J, Robinson TJ, et al.´ 2017 Recombination correlates with synaptonemal complex length and chromatin loop size in bovids—insights into mammalian meiotic chromosomal organization. Chromosoma 126:615–631. [PubMed: 28101670]

Sandor C, Li W, Coppieters W, Druet T, Charlier C, and Georges M. 2012 Genetic variants in REC8, RNF212, and PRDM9 influence male recombination in cattle. PLoS Genet. 8:e1002854.

Santucci-Darmanin S, Walpita D, Lespinasse F, Desnuelle C, Ashley T, and Paquis-Flucklinger V. 2000 MSH4 acts in conjunction with mlh1 during mammalian meiosis. FASEB J. 14:1539–1547. [PubMed: 10928988]

Schmekel K, and Daneholt B. 1995 The central region of the synaptonemal complex revealed in three dimensions. Trends Cell Biol. 5:239–242. [PubMed: 14732128]

Schramm S, Fraune J, Naumann R, Hernandez-Hernandez A, Höög C, Cooke HJ, Alsheimer M, and Benavente R. 2011 A novel mouse synaptonemal complex protein is essential for loading of central element proteins, recombination, and fertility. PLoS Genet. 7:e1002088.

Schrider DR, Hourmozdi JN, and Hahn MW. 2011 Pervasive multinucleotide mutational events in eukaryotes. Curr. Biol 21:1051–1054. [PubMed: 21636278]

Scornavacca C, and Galtier N. 2017 Incomplete lineage sorting in mammalian phylogenomics. Syst. Biol 66:112–120. [PubMed: 28173480]

Segura J, Ferretti L, Ramos-Onsins S, Capilla L, Farré M, Reis F, Oliver-Bonet M, Fernández-Bellón H, Garcia F, Garcia-Caldés M, et al. 2013 Evolution of recombination in eutherian mammals: insights into mechanisms that affect recombination rates and crossover interference.Proc. R. Soc. Lond. B 280:20131945.

Shen B, Jiang J, Seroussi E, Liu GE, and Ma L. 2018 Characterization of recombination features and the genetic basis in multiple cattle breeds.BMC Genom. 19:304.

Smith NG, and Eyre-Walker A. 2002 Adaptive protein evolution in Drosophila. Nature 415:1022. [PubMed: 11875568]

Smukowski C, and Noor M. 2011 Recombination rate variation in closely related species. Heredity 107:496. [PubMed: 21673743]

Snowden T, Acharya S, Butz C, Berardini M, and Fishel R. 2004 hMSH4hMSH5 recognizes Holliday junctions and forms a meiosis-specific sliding clamp that embraces homologous chromosomes. Mol. Cell 15:437–451. [PubMed: 15304223]

Stanzione M, Baumann M, Papanikos F, Dereli I, Lange J, Ramlal A, Tränkner D, Shibuya H, de Massy B, Watanabe Y, et al. 2016 Meiotic DNA break formation requires the unsynapsed chromosome axis-binding protein IHO1 (CCDC36) in mice. Nat. Cell Biol 18:1208. [PubMed: 27723721]

Stapley J, Feulner PG, Johnston SE, Santure AW, and Smadja CM. 2017 Variation in recombination frequency and distribution across eukaryotes: patterns and processes. Philos. Trans. R .Soc.B372:20160455. Stoletzki, N., and A. Eyre-Walker. 2010. Estimation of the neutrality index. Mol. Biol. Evol 28:63–70.

Stracker TH, and Petrini JH. 2011 The MRE11 complex: starting from the ends. Nat. Rev. Mol. Cell Biol 12:90. [PubMed: 21252998]

Swanson WJ, and Vacquier VD. 2002 The rapid evolution of reproductive proteins. Nat. Rev. Gen 3:137.

Swanson WJ, Nielsen R, and Yang Q. 2003 Pervasive adaptive evolution in mammalian fertilization proteins. Mol. Biol. Evol 20:18–20. [PubMed: 12519901]

Tarsounas M, Morita T, Pearlman RE, and Moens PB. 1999 RAD51 and DMC1 form mixed complexes associated with mouse meiotic chromosome cores and synaptonemal complexes. J. Cell Biol 147:207–220. [PubMed: 10525529]

Thomas J .Emerson H,RO,and Shendure J. 2009Extraordinarymolecular evolution in the PRDM9 fertility gene. PloS One 4:e8505.

Thorvaldsdóttir H, Robinson JT, and Mesirov JP. 2013 Integrative genomics viewer (IGV): high-performance genomics data visualization and exploration. Briefings Bioinform. 14:178–192.

Trapnell C, Pachter L, and Salzberg SL. 2009 TopHat: discovering splice junctions with RNA-Seq. Bioinformatics 25:1105–1111. [PubMed: 19289445]

Venkat A, Hahn MW, and Thornton JW. 2018 Multinucleotide mutations cause false inferences of lineage-specific positive selection. Nat. Ecol. Evol 2:1280. [PubMed: 29967485]

Ward JO, Reinholdt LG, Motley WW, Niswander LM, Deacon DC,Griffin LB, Langlais KK, Backus VL, Schimenti KJ, O'Brien MJ, et al. 2007 Mutation in mouse Hei10, an E3 ubiquitin ligase, disrupts meiotic crossing over. PLoS Genet. 3:e139.

Wheeler DL, Barrett T, Benson DA, Bryant SH, Canese K, Chetvernin V, Church DM, DiCuccio M, Edgar R, Federhen S, et al. 2006 Database resources of the national center for biotechnology information. Nucleic Acids Res. 35(Suppl. 1):D5–D12. [PubMed: 17170002]

Winkel K, Alsheimer M, Öllinger R, and Benavente R. 2009 Protein¨ SYCP2providesalinkbetweentransversefilamentsandlateralelements of mammalian synaptonemal complexes. Chromosoma 118:259–267. [PubMed: 19034475]

Wojtasz L, Cloutier JM, Baumann M, Daniel K, Varga J, Fu J, Anastassiadis K, Stewart AF, Reményi A, Turner JM, et al. 2012 Meiotic DNA double-strand breaks and chromosome asynapsis in mice are monitored by distinct HORMAD2-independent and-dependent mechanisms. Genes Dev. 26:958–973. [PubMed: 22549958]

Xu H, Beasley MD, Warren WD, van der Horst GT, and McKay MJ. 2005 Absence of mouse REC8 cohesin promotes synapsis of sister chromatids in meiosis. Dev. Cell 8:949–961. [PubMed: 15935783]

Xu Y, Greenberg RA, Schonbrunn E, and Wang PJ. 2017 Meiosis-specific proteins MEIOB and SPATA22 cooperatively associate with the single-stranded DNA-binding replication protein A complex and DNA double-strand breaks. Biol. Reprod 96:1096–1104. [PubMed: 28453612]

Yang F, de La Fuente R, Leu NA, Baumann C, McLaughlin KJ, and Wang PJ. 2006 Mouse SYCP2 is required for synaptonemal complex assembly and chromosomal synapsis during male meiosis. J. Cell Biol 173:497–507. [PubMed: 16717126]

Yang F, Gell K, Van Der Heijden GW, Eckardt S, Leu NA, Page DC, Benavente R, Her C, Höög C, McLaughlin KJ, et al. 2008 Meiotic failure in male mice lacking an X-linked factor. Genes Dev. 22:682–691. [PubMed: 18316482]

Yang F, Silber S, Leu NA, Oates RD, Marszalek JD, Skaletsky H, Brown LG, Rozen S, Page DC, and Wang PJ. 2015 Tex11 is mutated in infertile men with azoospermia and regulates genome-wide recombination rates in mouse. EMBO Mol. Med 7:1198–1210. [PubMed: 26136358]

Yang Z 1997 Paml: a program package for phylogenetic analysis by maximum likelihood. Bioinformatics 13:555–556.

Yang Z 2007 Paml 4: Phylogenetic analysis by maximum likelihood. Mol. Biol. Evol 24:1586–1591. [PubMed: 17483113]

Zerbino DR, Achuthan P, Akanni W, Amode MR, Barrell D, Bhai J, Billis K, Cummins C, Gall A, Girón CG, et al. 2017 Ensembl 2018. Nucleic Acids Res. 46(D1):D754–D761.

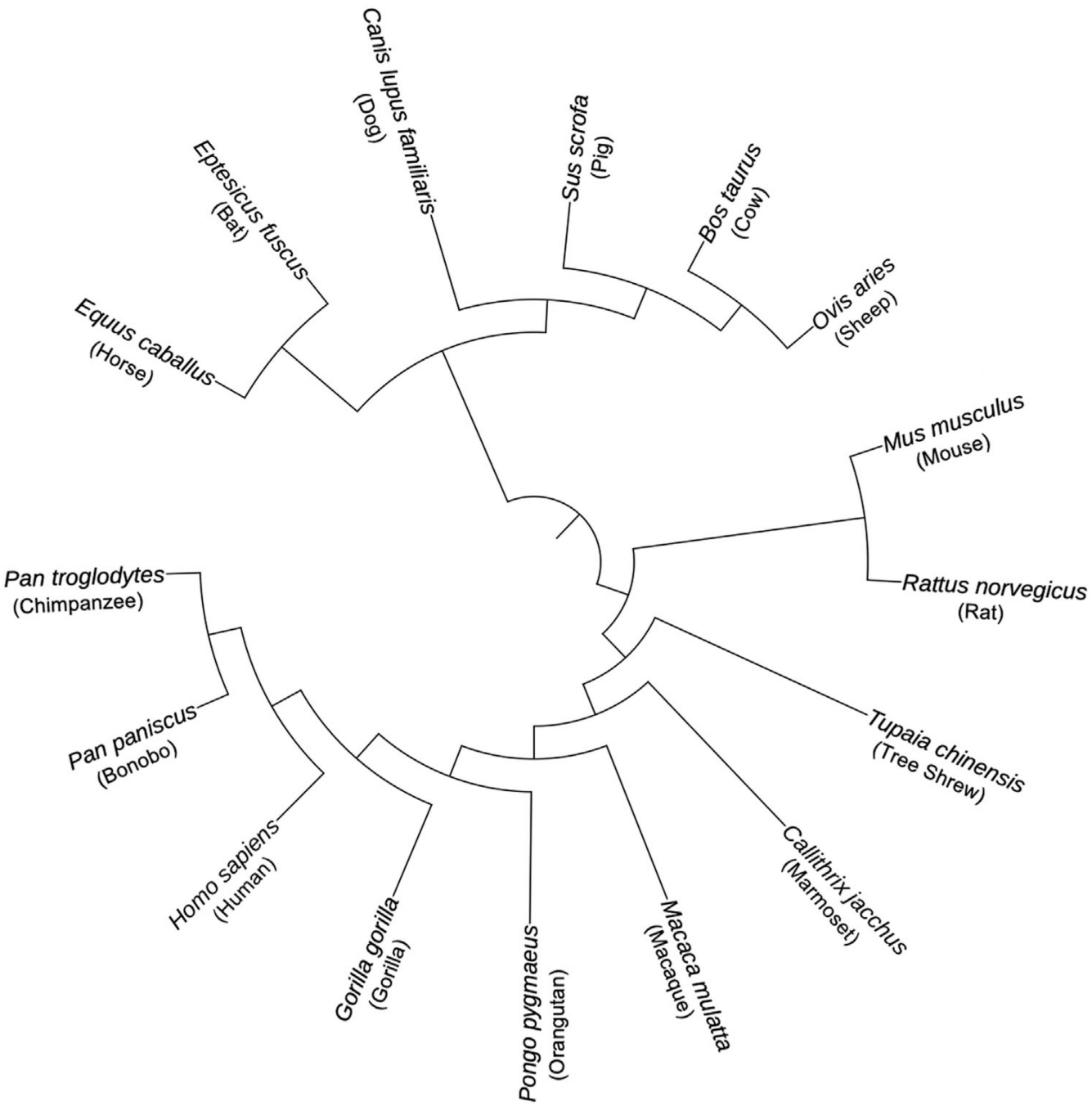

Figure 1.

Species tree assumed in analyses of molecular evolution.

Note: Figure generated using Letunic and Bork (2019).

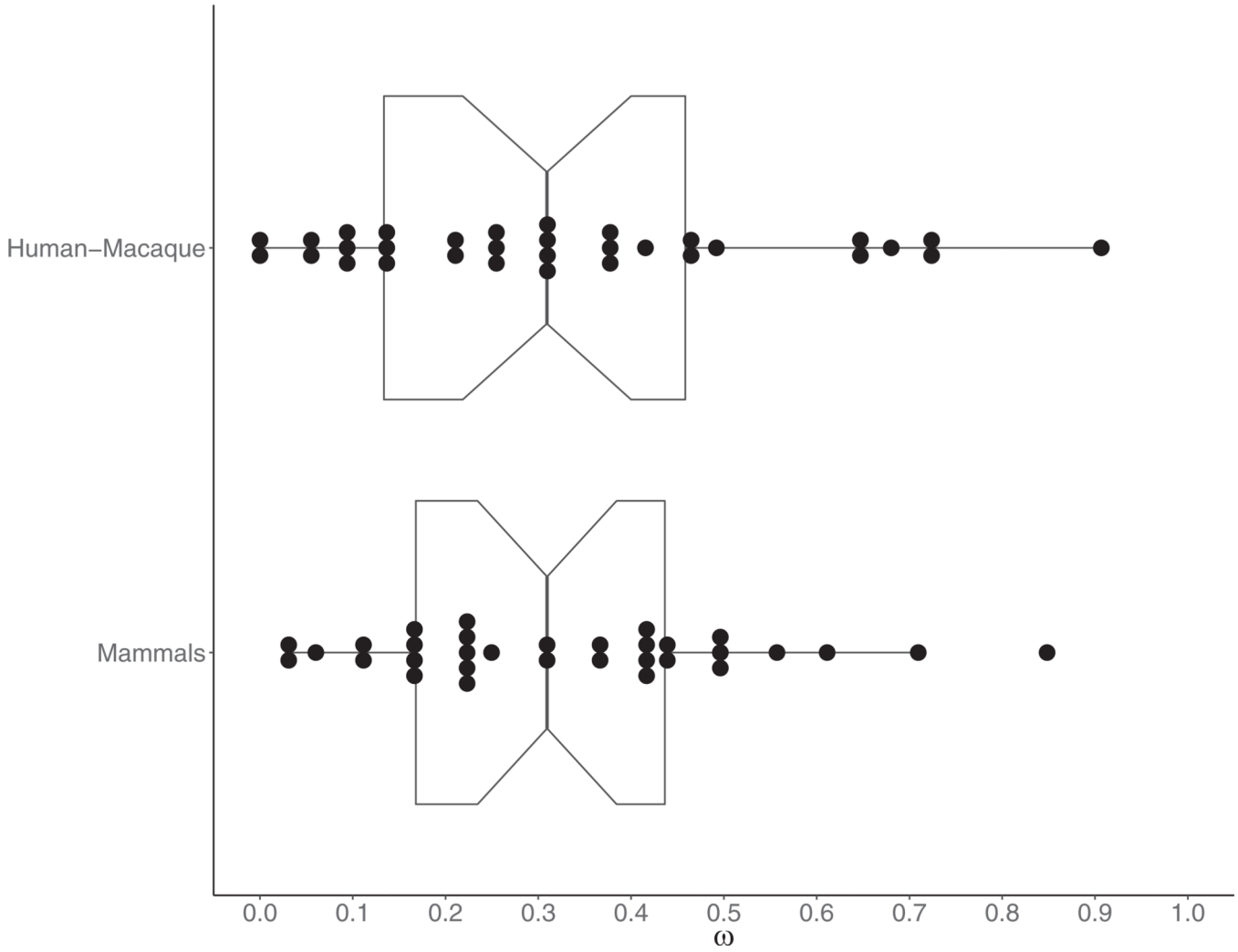

Figure 2.
Distribution of ω for 32 recombination genes. (A) Mammals: divergence estimated across the mammalian phylogeny. (B) Human–Macaque: pairwise divergence between human and macaque.

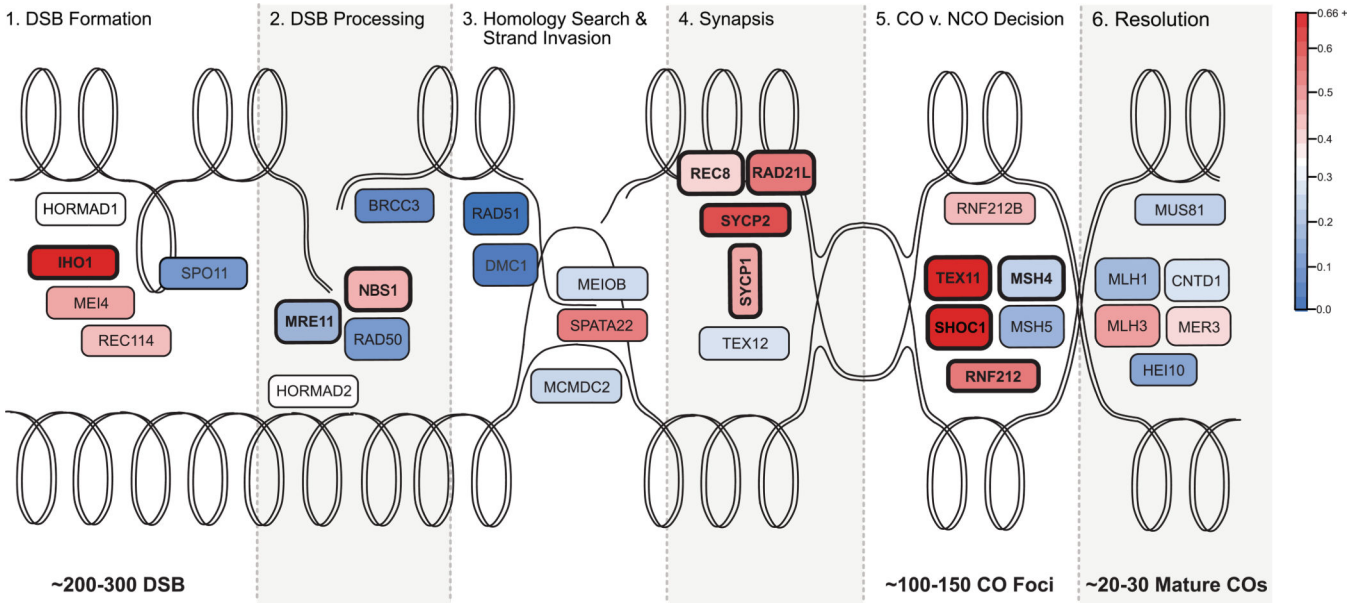

Figure 3.

Evolutionary rate of key recombination genes in the context of the recombination pathway. The double lines represent the looped dsDNA of two homologous chromosomes, one oriented across the top of the figure and the other across the bottom. Each panel, from left to right, illustrates the progression of a homologous recombination event. The process starts with hundreds DSBs throughout the genome, a fraction of which are ultimately resolved as mature crossovers. Additional information about each gene can be found in Table 1. The color of each gene represents its evolutionary rate relative to the average for recombination genes ($\omega = 0.3275$): more rapidly evolving genes are depicted in darker shades of red and more conserved genes are depicted in darker shades of blue. The corresponding estimates of the evolutionary rate of each gene are reported in Table 3. Genes that exhibit a signature of positive selection are in bold.

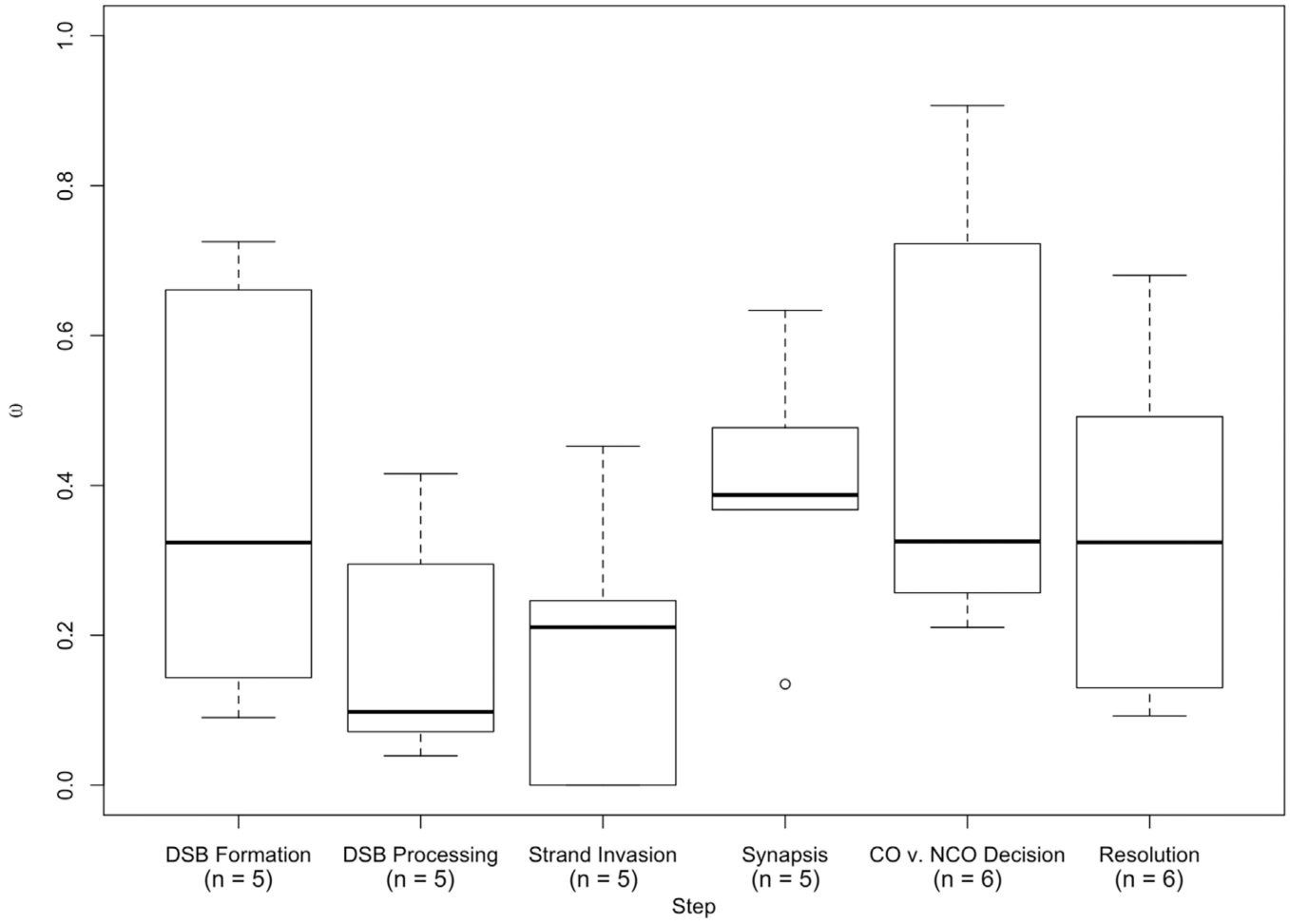

Figure 4.
Boxplot of ω by step in recombination pathway.

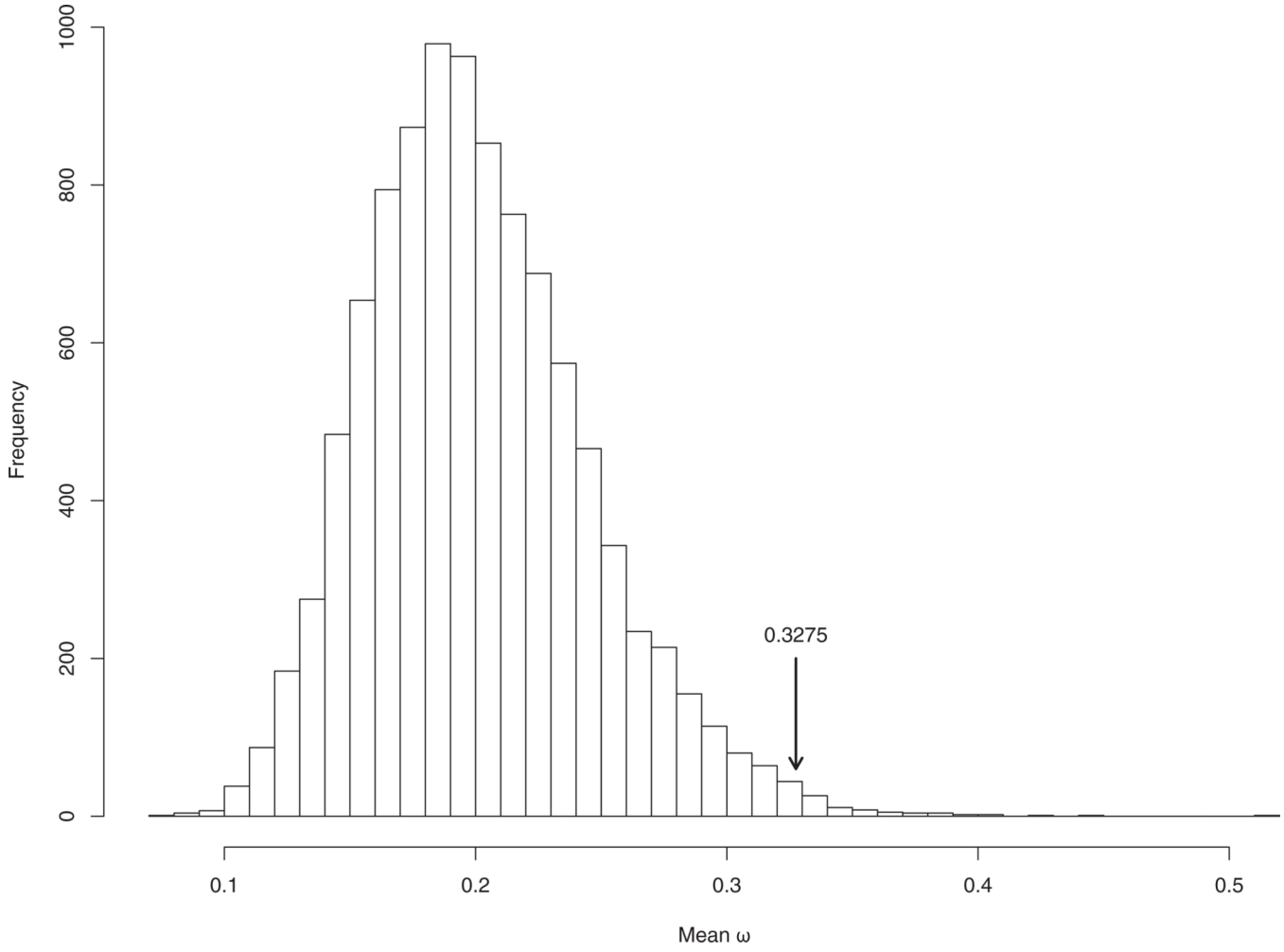

Figure 5.

Distribution of average divergence (ω) between human and macaque of 10,000 gene sets randomly drawn from the entire genome. Average ω among these random draws was observed to be equal to or greater than that observed among recombination genes less than 1% of the time ($P = 0.0075$).

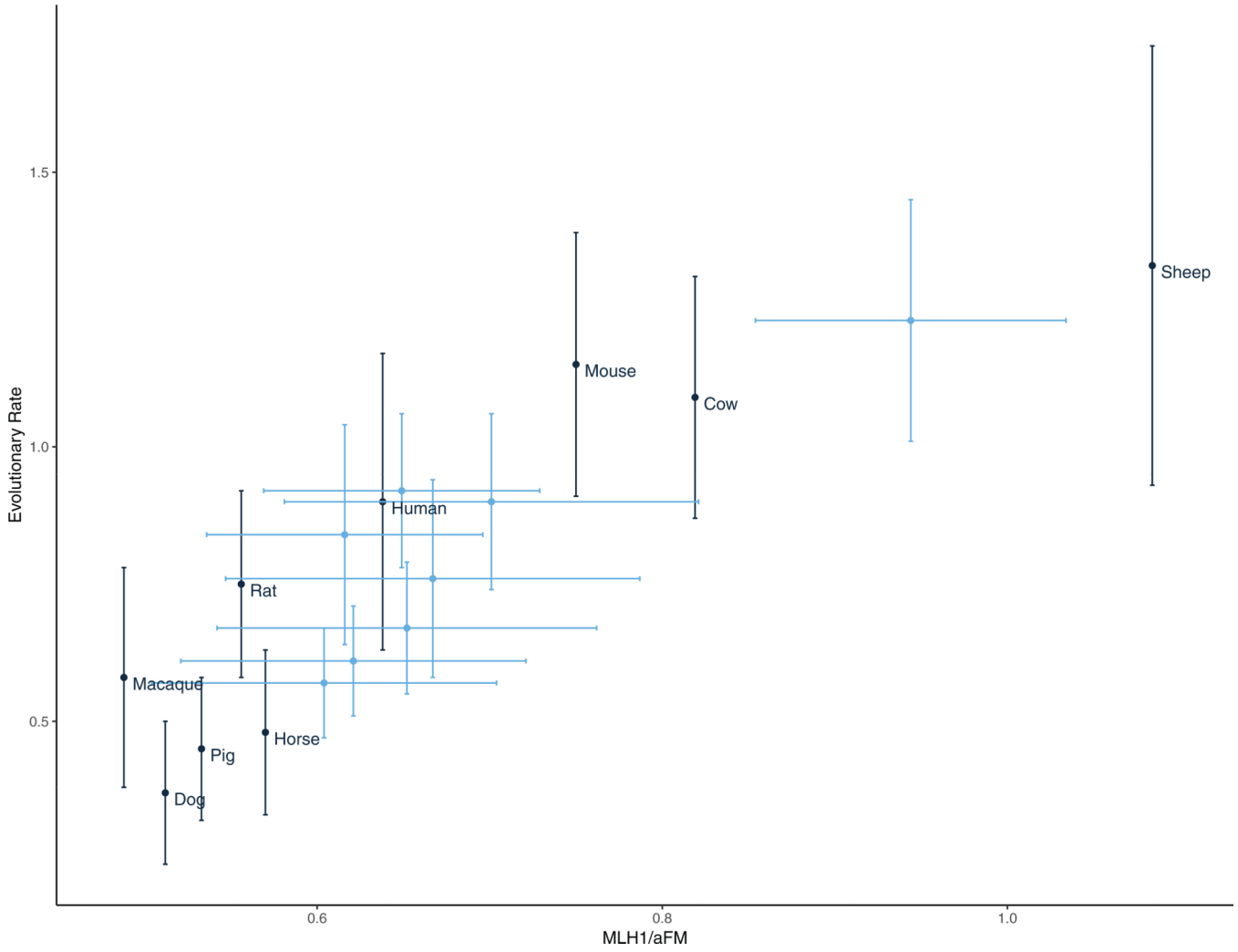

Figure 6.

The rate of evolution of *TEX11* and recombination rate (*MLH1*/aFN) are correlated across the mammalian phylogeny. Black: Point estimates of recombination rate (derived from published estimates of *MLH1* foci per cell—see Table S7) and the estimated rate of evolution of *TEX11* in the terminal branch. Blue: Ancestrally reconstructed estimates of recombination rate and evolutionary rate for internal nodes. Error bars represent ±1SD.

Table 1.

List of 32 genes surveyed, organized by step in the recombination pathway, including function in meiosis and direct interactions with other genes surveyed.

Gene	Complex	Function	Direct Interaction	Citation
(A) Double strand break formation				
HORMAD1		Associates with unsynapsed chromosomes, required for accumulation of MCD recombinosomes	*IHO1*	Fukuda et al. (2010)
MEI4	MCD Recombinosome	Component of a complex that promotes DSB formation by activating SPO11	*REC114*	Kumar et al. (2010)
REC114	MCD Recombinosome	Component of a complex that promotes DSB formation by activating SPO11	*MEI4, IHO1*	Kumar et al. (2018)
IHO1/CCDC36	MCD Recombinosome	Component of a complex that promotes DSB formation by activating SPO11	*REC114, HORMAD1*	Stanzione et al. (2016)
SPO11		Generates double strand breaks		Romanienko and Camerini-Otero (2000)
(B) Double strand break processing				
HORMAD2		Associates with unsynapsed chromosomes, detects chromosome asynapsis		Wojtasz et al. (2012)
MRE11	MRN complex	Part of complex that processes newly formed DSB, trims off *SPO11*	*NBS1, RAD50*	Stracker and Petrini (2011)
NBS1	MRN complex	Part of complex that processes newly formed DSB, responsible for nuclear localization of the complex	*MRE11, RAD50*	Oh et al. (2016)
RAD50	MRN complex	Part of complex that processes newly formed DSB, holds broken DNA ends together	*NBS1, MRE11*	Lamarche et al. (2010)
BRCC3		Involved in DNA repair		Dumont and Payseur (2011)
(C) Homology search and strand invasion				
DMC1		Mediates/catalyzes homologous chromosome pairing	*RAD51*	Tarsounas et al. (1999)
RAD51		Mediates/catalyzes homologous chromosome pairing	*DMC1*	Cloud et al. (2012)
SPATA22		Required for the completion of strand invasion	*MEIOB*	Xu et al. (2017)
MEIOB		Required for the completion of strand invasion	*SPATA22*	Luo et al. (2013)
MCMDC2		Required for the formation or stabilization of DNA strand invasion events		Finsterbusch et al. (2016)
(D) Synapsis				
REC8	Cohesion complex	Maintains sister-chromatid cohesion		Xu et al. (2005)
RAD21L	Cohesion complex	Maintains sister-chromatid cohesion, initiates synapsis		Lee and Hirano (2011)
SYCP1	Synaptonemal complex	Binds homologous chromosomes, transverse filament	*SYCP2*	de Vries et al. (2005)

Gene	Complex	Function	Direct Interaction	Citation
SYCP2	Synaptonemal complex	Binds homologous chromosomes, lateral element	*SYCP1, TEX11*	Winkel et al. (2009)
TEX12	Synaptonemal complex	Binds homologous chromosomes, central element		Hamer et al. (2006)
(E) Crossover/non-crossover decision				
TEX11		Required for the recruitment of proteins that designate crossovers	*SYCP2, SHOC1*	Yang et al. (2008)
SHOC1		Required for the recruitment of proteins that designate crossovers	*TEX11*	Guiraldelli et al. (2018)
RNF212		Selectively localizes to a subset of DSB, stabilizing *MSH4/MSH5*	mutS Complex	Reynolds et al. (2013)
RNF212B		Paralog of *RNF212* associated with within species variation in recombination rate		Kadri et al. (2016)
MSH4	mutS complex	Localizes to a subset of DSB, regulating crossover number	*MSH5*	Santucci-Darmanin et al. (2000)
MSH5	mutS complex	Localizes to a a subset of DSB, regulating crossover number	*MSH4*	de Vries et al. (1999)
(F) Resolution				
MER3/HFM1		Required for correct localization of *MLH1* and crossover formation		Guiraldelli et al. (2013)
CNTD1		Required crossover maturation and recruitment of *HEI10* and *MLH1/MLH3*	*HEI10*, mutL Complex	Holloway et al. (2014)
HEI10/CCNB1IP1		Antagonistically regulates RNF212 activity	*RNF212*	Qiao et al. (2014)
MLH1	mutL complex	Mismatch repair gene that localizes to and resolves crossovers	*MLH3*	Baker et al. (1996)
MLH3	mutL complex	Mismatch repair gene that localizes to and resolves crossovers	*MLH1*	Lipkin et al. (2002)
MUS81		Generates a subset of *MLH1/MLH3*-independent crossovers		Holloway et al. (2008)

Note: Genes in bold have been associated with interindividual differences in recombination rate in at least one species of mammals.

Table 2.

Six PAML site models used to measure evolutionary rate and test for positive selection.

Model	Site Classes	ω Range	Positive Selection?
0	1	<1	No
1	2	< 1,= 1	No
2	3	< 1,= 1,>1	Yes
7	10	0 − 1	No
8	11	0− 1,>1	Yes
8a	6	0 − 1,= 1	No

Note: Models varied in the number of ω classes, the range of ω for each of these classes, and whether a class of sites subject to positive selection was included.

Table 3.

Evolutionary rates and tests for positive selection across mammals at 32 recombination genes.

Gene	bp	*N*	ω	M	M1—M2	*P*	M7—M8	*P*	M8a—M8	*P*	BEB
(A) DSB formation											
HORMAD1	1212	16	0.3036	7	0	1.000	1.795	0.4076	—	—	0
MEI4	1170	16	0.4332	7	0	1.000	0.005	0.9976	—	—	0
REC114	870	15	0.4003	7	0	1.000	5.384	0.0677	—	—	0
IHO1	1824	16	0.7095	**8**	13.061	**0.0015**	17.571	**0.0002**	14.527	**0.0001**	**1**
SPO11	1188	15	0.1654	7	0	1.000	4.648	0.0980	—	—	0
(B) DSB processing											
HORMAD2	981	15	0.3153	7	0	1.000	3.650	0.1612	—	—	0
MRE11	2136	16	0.1688	**8**	0.363	0.8342	11.931	**0.0026**	4.706	**0.0301**	0
NBS1	2289	15	0.4183	**8**	0	1.000	12.763	**0.0017**	4.087	**0.0432**	0
RAD50	3936	16	0.1006	7	0	1.000	0.301	0.8605	—	—-	0
BRCC3	954	15	0.0602	7	0	1.000	0.250	0.8826	—	—	0
(C) Homology search and strand invasion											
DMC1	1020	15	0.0351	1	0.488	0.7835	5.000	0.0821	—	—	**1**
RAD51	1017	16	0.0268	7	0	1.000	0	1.000	—	—	0
SPATA22	1101	16	0.4893	7	0	1.000	0.429	0.8070	—	—	0
MEIOB	1425	16	0.2341	7	0	1.000	0.665	0.7172	—	—	0
MCMDC2	2052	16	0.2239	7	0	1.000	0.628	0.7307	—	—	0
(D) Synapsis											
REC8	1833	16	0.3698	**8**	0	1.000	14.690	**0.0006**	5.927	**0.0149**	0
RAD21L	1686	15	0.503	**8**	12.124	**0.0023**	32.050	<**0.0001**	12.049	**0.0005**	**4**
SYCP1	3015	16	0.4337	**8**	8.711	**0.0128**	26.860	<**0.0001**	9.243	**0.0024**	**3**
SYCP2	4650	16	0.5572	**8**	11.584	**0.0031**	37.200	<**0.0001**	15.838	**0.0001**	0
TEX12	369	14	0.2297	7	0.0565	0.9721	1.549	0.4610	—	—	0
(E) CO/NCO decision											
TEX11	2844	15	0.8483	**8**	60.872	<**0.0001**	82.665	<**0.0001**	61.141	<**0.0001**	**14**
SHOC1	4644	16	0.6113	**8**	12.447	**0.0020**	30.561	<**0.0001**	15.645	**0.0001**	0
RNF212	948	16	0.5014	**8**	0	1.000	16.366	**0.0003**	5.202	**0.0226**	**1**

Gene	bp	*N*	ω	M	M1—M2	*P*	M7—M8	*P*	M8a—M8	*P*	BEB
RNF212B	906	14	0.4066	7	0	1.000	0.500	0.7788	—	—	0
MSH4	2814	16	0.2132	**8**	16.608	**0.0002**	39.447	<**0.0001**	23.238	<**0.0001**	**6**
MSH5	2565	15	0.1642	7	0	1.000	4.214	0.1216	—	—	0
(F) Resolution											
MER3	4458	16	0.3633	8a	0	1.000	12.838	**0.0016**	3.109	0.0779	0
CNTD1	1026	15	0.2496	7	0	1.000	0.936	0.6263	—	—	0
HEI10	831	15	0.1226	7	0	1.000	0.250	0.8826	—	—	0
MLH1	2313	15	0.1652	8a	0	1.000	12.221	**0.0022**	0.280	0.5970	0
MLH3	4419	16	0.4444	7	0	1.000	3.757	0.1528	—	—	0
MUS81	1665	16	0.2124	7	0	1.000	0.628	0.7304	—	—	0

Note: bp, length of alignment; *N*, number of sequences; ω, estimated rate of evolution using the model of best fit; M, model of best fit; M1–M2, log-likelihood of M2 over M1; M7–M8, log-likelihood of M8 over M7; M8a–M8, log-likelihood of M8 over M8a; BEB, number of individual amino acids with BEB; $P > 0.95$.

Table 4.

Comparisons of polymorphism within humans to divergence between human and macaque at recombination genes.

Gene	ω	Pn	Ps	Pn/Ps	Dn	Ds	Dn/Ds	MK Test	*NI*	*DoS*	Direction
(A) DSB formation											
HORMAD1	0.0901	43	10	4.3	5	12	0.4167	**0.0002**	10.32	−0.5172	Neg.
MEI4	0.7252	9	2	4.5	24	9	2.6667	0.7013	1.6875	−0.0909	—
REC114	0.3239	49	21	2.3333	11	14	0.7857	**0.02949**	2.9700	−0.2600	Neg.
IHO1	0.6608	72	28	2.5714	36	19	1.8947	0.4658	1.3571	−0.0645	—
SPO11	0.1434	62	28	2.2143	11	22	0.5000	**0.0008**	4.4286	0.3556	Neg.
(B) DSB processing											
HORMAD2	0.295	50	16	3.125	7	9	0.7778	0.0177	4.0179	−0.3201	Neg.
MRE11	0.0392	139	48	2.8958	5	35	0.1429	<**0.0001**	20.2708	−0.6183	Neg.
NBS1	0.4155	119	58	2.0517	34	25	1.3600	0.2086	1.5086	−0.0960	—
RAD50	0.0714	168	55	3.0517	8	43	0.1860	<**0.0001**	16.4182	−0.5965	Neg.
BRCC3	0.0979	7	12	0.5833	2	6	0.3333	0.6758	1.7500	−0.1184	—
(C) Homology search and strand invasion											
DMC1	0.000	43	25	1.72	0	11	0.0000	<**0.0001**	—	−0.6324	Neg.
RAD51	0.000	27	29	0.9310	0	13	0.0000	**0.0010**	—	−0.4821	Neg.
SPATA22	0.4523	67	26	2.5769	21	10	2.1000	0.6535	1.2271	−0.0430	—
MEIOB	0.2462	45	17	2.6471	20	22	0.9091	**0.0094**	2.9118	−0.2496	Neg.
MCMDC2	0.2108	90	24	3.7500	16	26	0.6154	<**0.0001**	6.0938	−0.4085	Neg.
(D) Synapsis											
REC8	0.477	90	45	2.000	38	31	1.2258	0.1264	1.6316	−0.1159	—
RAD21L	0.6334	21	6	3.500	27	13	2.0769	0.4176	1.6852	−0.1028	—
SYCP1	0.3676	122	60	2.033	33	37	1.2222	0.1204	1.6636	−0.1203	—
SYCP2	0.3676	246	87	2.8276	74	53	1.3962	**0.0015**	2.0252	−0.1561	Neg.
TEX12	0.1349	15	9	1.6667	2	4	0.5000	0.3598	3.3333	−0.2917	—
(E) CO/NCO decision											
TEX11	0.9068	78	45	1.7333	55	25	2.200	0.4541	0.7879	0.05335	—
SHOC1	0.7225	227	72	3.1528	85	37	2.2973	0.2199	1.3724	−0.0625	—
RNF212	0.387	—	—	—	17	18	0.9444	—	—	—	—

Gene	ω	Pn	Ps	Pn/Ps	Dn	Ds	Dn/Ds	MK Test	*NI*	*DoS*	Direction
RNF212B	0.2566	9	3	3.000	8	12	0.6667	0.0759	4.5000	−0.3500	—
MSH4	0.2635	149	50	2.9800	24	29	0.8276	<**0.0001**	3.6008	−0.2959	Neg.
MSH5	0.2106	129	64	2.0156	19	33	0.5758	**0.0001**	3.5008	−0.3030	Neg.
(F) Resolution											
MER3	0.3247	236	92	2.5652	54	44	1.2273	**0.0029**	2.0902	−0.1685	Neg.
CNTD1	0.6803	56	29	1.9310	13	8	1.6250	0.8001	1.1883	−0.0398	—
HEI10	0.3235	50	21	2.3810	4	5	0.8000	0.1417	2.9762	−0.2598	—
MLH1	0.0924	161	48	3.3542	9	29	0.3103	<**0.0001**	10.8079	−0.5335	Neg.
MLH3	0.4919	252	90	2.8	77	57	1.3509	**0.0009**	2.0727	−0.1622	Neg.
MUS81	0.1299	129	49	2.6327	17	40	0.4250	<**0.0001**	6.1945	0.4265	Neg.

Note: Pn, number of nonsynonymous polymorphisms; Ps, number of synonymous polymorphisms; Dn, number of nonsynonymous substitutions; Ds, number of synonymous substitutions; MK Test, P value of the McDonald-Kreitman test

Table 5.

Evolutionary rates and tests for positive selection across mammals at recombination genes after removal of potential MNMs.

Gene	bp	*N*	ω	M	M1–M2	*P*	M7–M8	*P*	M8a–M8	*P*
IHO1	1824	16	0.6104	7	0	1.000	0.258	0.8789	—	—
MRE11	2136	16	0.1330	7	0.226	0.8930	3.056	*0.2169*	—	—
NBS1	2289	15	0.3413	7	0	1.000	1.956	0.3761	—	—
REC8	1833	16	0.2905	7	0	1.000	5.321	0.0699	—	—
RAD21L	1686	15	0.4271	8a	2.329	0.3121	9.497	**0.0087**	1.620	0.2031
SYCP1	3015	16	0.3731	8a	3.328	0.1893	13.440	**0.0012**	2.122	0.1452
SYCP2	4650	16	0.4752	7	0	1.000	1.758	0.4151	—	—
TEX11	2844	15	0.7287	**8**	9.989	**0.0068**	18.776	**0.0001**	10.656	**0.0011**
SHOC1	4644	16	0.5519	8a	0	1.000	7.439	**0.0242**	0.292	0.5887
RNF212	948	16	0.3685	7	0	1.000	0	1.000	—	—
MSH4	2814	16	0.1509	7	0	1.000	2.079	0.3536	—	—

Note: bp, length of alignment; *N*, number of sequences; ω, estimated rate of evolution using the model of best fit; M, model of best fit; M1–M2, log-likelihood of M2 over M1; M7–M8, log-likelihood of M8 over M7; M8a–M8, log-likelihood of M8 over M8a.

Table 6.

Comparison of proportion of positively selected genes by step in the recombination pathway: (A) DSB formation, (B) DSB processing, (C)homology search and strand invasion, (D) synapsis, (E) CO/NCO decision, and (F) resolution.

	Focal Steps		Other Steps		Fisher's Exact Test
Focal Step(s)	**Yes**	**No**	**Yes**	**No**	***P*-Value**
A	1	4	10	17	0.6367
B	2	3	9	18	1.0000
C	0	4	11	17	0.1378
D	4	1	7	20	0.0367
D	4	2	7	19	0.1476
F	0	6	11	15	0.0711
A, B	3	7	8	14	1.0000
B, C	2	8	9	13	0.4250
C, D	4	6	7	15	0.7020
D, E	8	3	3	18	**0.0018**
E, F	4	6	7	15	1.0000

Table 7.

Correlations between substitution rate and recombination rate, measured as the average number of MLH1 foci per cell divided by the autosomal fundamental number (aFN), across 9 species of mammals for 31 recombination genes.

	Correlation Coefficient			Partial Correlation Coefficient		
Gene	**dS–ω**	**dS–MLH1**	**ω–MLH1**	**dS–ω**	**dS–MLH1**	**ω–MLH1**
(A) DSB formation						
HORMAD1	0.908(**0.98**)	0.753(0.93)	0.734(0.92)	0.692(0.92)	0.258(0.67)	0.201(0.63)
MEI4	−0.81(**0.037**)	0.17(0.64)	−0.188(0.37)	−0.809(**0.043**)	0.0399(0.52)	−0.0701(0.45)
REC114	−0.608(**0.14**)	0.659(**0.95**)	−0.517(0.18)	−0.459(0.22)	0.21(0.66)	−0.281(0.32)
IHO1	0.52(0.84)	0.273(0.77)	0.328(0.72)	0.531(0.84)	0.0413(0.54)	0.223(0.64)
SPO11	0.511(0.82)	−0.087(0.42)	−0.0323(0.47)	0.606(0.87)	−0.0212(0.49)	−0.00137(0.5)
(B) DSB processing						
HORMAD2	0.0159(0.49)	0.672(0.92)	−0.121(0.44)	0.146(0.6)	0.482(0.82)	−0.224(0.35)
MRE11	−0.451(0.18)	−0.0115(0.53)	0.212(0.64)	−0.338(0.23)	0.0897(0.6)	0.23(0.66)
NBS1	−0.693(0.078)	0.0764(0.57)	−0.206(0.34)	−0.719(0.062)	−0.112(0.41)	−0.216(0.35)
RAD50	−0.375(0.23)	0.23(0.73)	−0.0193(0.48)	−0.409(0.21)	0.193(0.68)	0.0858(0.56)
BRCC3	0.112(0.58)	−0.123(0.38)	−0.145(0.4)	0.103(0.5	−0.0493(0.46)	−0.139(0.42)
(C) Homology search and strand invasion						
DMC1	0.307(0.68)	0.441(0.81)	0.156(0.6)	0.294(0.67)	0.245(0.67)	0.0264(0.52)
RAD51	−0.0234(0.49)	−0.0766(0.43)	−0.0617(0.46)	−0.0255(0.48)	−0.0348(0.48)	−0.0651(0.47)
SPATA22	−0.143(0.4)	0.0484(0.52)	−0.215(0.37)	−0.105(0.44)	0.00682(0.51)	−0.204(0.39)
MEIOB	0.274(0.67)	−0.604(0.053)	−0.263(0.33)	0.2(0.62)	−0.285(0.29)	−0.161(0.4)
MCMDC2	−0.448(0.2)	0.275(0.75)	−0.22(0.35)	−0.426(0.22)	0.112(0.59)	−0.121(0.42)
(D) Synapsis						
REC8	−0.528(0.17)	0.404(0.85)	−0.0632(0.44)	−0.608(0.13)	0.331(0.74)	0.205(0.64)
RAD21L	−0.691(0.077)	−0.374(0.2)	0.474(0.81)	−0.657(0.1)	0.136(0.59)	0.388(0.74)
SYCP1	−0.0469(0.47)	0.235(0.73)	0.0762(0.54)	−0.0569(0.46)	0.147(0.63)	0.0914(0.56)
SYCP2	0.269(0.69)	0.117(0.61)	0.199(0.64)	0.314(0.71)	0.0328(0.53)	0.177(0.61)
TEX12	0.118(0.57)	0.485(0.79)	−0.00613(0.49)	0.171(0.61)	0.307(0.7)	−0.0541(0.47)
(E) CO/NCO decision						
TEX11	0.227(0.67)	−0.073(0.49)	0.725(**0.96**)	0.42(0.82)	−0.316(0.25)	0.756(**0.96**)

	Correlation Coefficient			Partial Correlation Coefficient		
Gene	**dS–ω**	**dS–MLH1**	**ω–MLH1**	**dS–ω**	**dS–MLH1**	**ω–MLH1**
SHOC1	−0.72(**0.046**)	−0.1(0.39)	0.221(0.67)	−0.767(**0.04**)	0.158(0.62)	0.243(0.65)
RNF212	0.0593(0.54)	−0.0702(0.44)	−0.0123(0.49)	0.0774(0.55)	−0.0418(0.46)	0.00075(0.5)
MSH4	−0.881(**0.011**)	0.189(0.67)	−0.163(0.37)	−0.907(**0.0033**)	0.0802(0.56)	0.0261(0.51)
MSH5	0.16(0.6)	−0.347(0.2)	−0.308(0.31)	0.103(0.57)	−0.143(0.39)	−0.287(0.32)
(F) Resolution						
MER3	−0.563(0.13)	−0.457(0.091)	0.395(0.77)	−0.529(0.15)	−0.101(0.41)	0.242(0.66)
CNTD1	−0.821(0.037)	0.0969(0.57)	−0.0135(0.5)	−0.837(**0.035**)	0.155(0.61)	0.121(0.59)
HEI10	−0.158(0.40)	0.0597(0.56)	0.107(0.56)	−0.189(0.38)	0.0746(0.56)	0.127(0.58)
MLH1	0.154(0.61)	0.133(0.63)	0.165(0.61)	0.167(0.61)	0.0747(0.56)	0.15(0.6)
MLH3	−0.125(0.41)	−0.117(0.38)	−0.119(0.41)	−0.131(0.41)	−0.0908(0.42)	−0.143 (0.4)
MUS81	0.358(0.74)	0.259(0.73)	0.244(0.67)	0.359(0.73)	0.0907(0.58)	0.171(0.6)

Note: The posterior probability is given in parentheses.